Bipolar spintronics: Fundamentals and applications

I. Žutić J. Fabian S. C. Erwin

By incorporating spin-dependent properties and magnetism in semiconductor structures, new applications can be considered which go beyond magnetoresistive effects in metallic systems. Notwithstanding the prospects for spin/magnetism-enhanced logic in semiconductors, many important theoretical, experimental, and materials challenges remain. Here we discuss the challenges for realizing a particular class of associated applications and our proposal for bipolar spintronic devices in which carriers of both polarities (electrons and holes) would contribute to spin-charge coupling. We formulate the theoretical framework for bipolar spin-polarized transport and describe several novel effects in two- and three-terminal structures which arise from the interplay between nonequilibrium spin and equilibrium magnetization.

Introduction

Magnetoresistive effects in metallic magnetic multilayers [1–13], such as giant magnetoresistance (GMR) and tunneling magnetoresistance (TMR), have already been successfully employed in a variety of device applications. Well-known examples include magnetic sensors, magnetic read heads in computer hard drives, and nonvolatile magnetic random access memory (MRAM); many of these are discussed in more detail in other papers in this issue. Much less effort has gone into exploring the potential use of semiconductors in spintronic applications. Spintronics, or spin electronics, involves the study of active control and manipulation of spin degrees of freedom in solid-state systems [13]. Conventionally, the term *spin* designates either the spin of a single electron, which can be detected by its magnetic moment, or the average spin of an ensemble of electrons, manifested by magnetization. The control of spin is then the control of either the population and the phase of the spin of an ensemble of particles, or the coherent spin manipulation of a single- or few-spin system.

The field of semiconductor spintronics [13–23] continues to grow rapidly, and in this paper it is not possible to cover it in its entirety. Here we focus on our proposal for bipolar spintronics [24–27] in semiconductor systems and briefly recall several challenges that must be overcome as well as important findings that could make

possible its practical realization. Use of the term *bipolar* indicates that carriers of both polarities (electrons and holes) are important [28]. In contrast to unipolar devices such as metallic spintronic devices [1, 2], bipolar devices exhibit large deviations from local charge neutrality and intrinsic nonlinearities in their current–voltage characteristics, which are important even at a small applied bias.

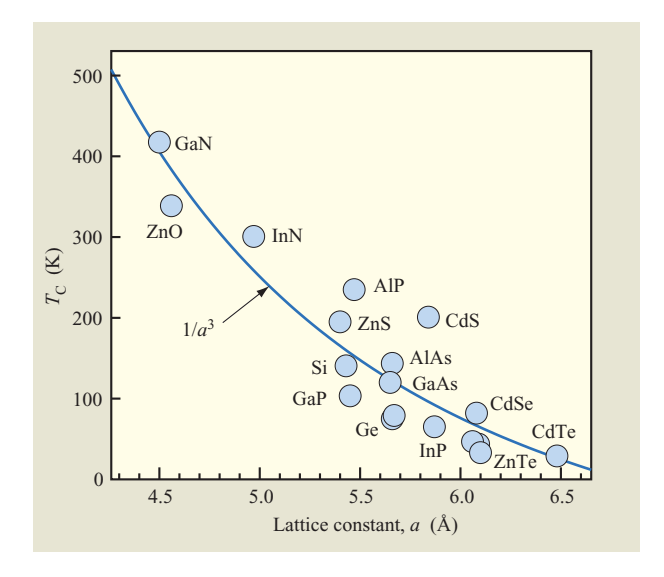
These characteristics, together with the ease of manipulating the minority charge carriers, make it possible to design active devices that can amplify signals as well as provide additional degrees of control not available in charge-based electronics. Analogous to bipolar charge transport [29, 30], which is dominated by the influence of the nonequilibrium carrier density, nonequilibrium spin density (unequal populations of "spin-up" and "spin-down" carriers) plays an important role in bipolar spintronics. We discuss here several implications of nonequilibrium spin density in semiconductors, such as spin capacitance, spin density amplification, spin-polarized solar battery, and the spin-voltaic effect, a spin analog of the photovoltaic effect.

The generation of nonequilibrium spin polarization (of carriers as well as nuclei) and nonequilibrium spin density in semiconductors has been known for several decades. By using methods such as optical orientation or optical pumping [31], the angular momentum of absorbed

©Copyright 2006 by International Business Machines Corporation. Copying in printed form for private use is permitted without payment of royalty provided that (1) each reproduction is done without alteration and (2) the Journal reference and IBM copyright notice are included on the first page. The title and abstract, but no other portions, of this paper may be copied or distributed royalty free without further permission by computer-based and other information-service systems. Permission to republish any other portion of this paper must be obtained from the Editor.

0018-8646/06/\$5.00 @ 2006 IBM





Predicted variation of the Curie temperature T_C with lattice constant a for various Mn-doped semiconductors, as given by the Zener model for carrier-mediated ferromagnetism. The curve is a fit to the predicted values. Adapted from Figure 16 and Tables I and II of [55], with permission; ©2001 American Physical Society.

circularly polarized light is transferred to the medium. Electron orbital momenta are directly oriented by light and, through spin-orbit interaction, electron spins become polarized. In a pioneering work, Lampel [32] demonstrated that spins in p-doped silicon can be optically oriented (polarized). Subsequent work also showed that the optical orientation can be used to establish electron spin polarization in n-doped GaAs [33, 34] and to provide a much higher spin polarization in direct-bandgap semiconductors than in silicon [31]. For example, electrical spin injection, a method for generating nonequilibrium spin, had already been realized in 1963 by Clark and Feher [35], who passed a direct current through a sample of InSb in the presence of a constant applied magnetic field. Motivated by this work and by the principle of optical orientation [31], Aronov and Pikus [36–38] established several key concepts in electrical spin injection from ferromagnets into metals, semiconductors, and superconductors.

At present, bipolar spin-polarized transport in semiconductors is mostly limited to low temperatures. Progress toward room-temperature operation will depend critically on the development of new materials. Moreover, researchers are currently pursuing two distinct approaches for operation at room temperature: 1) the use of hybrid structures that combine metallic ferromagnets and semiconductors; and 2) the use of all-semiconductor

structures. Each of these approaches has its own materials issues. In the first, the wide range of metallic ferromagnetic materials with high Curie temperature $T_{\rm C}$ provides a possible advantage. Interestingly, this advantage may not be fully realized in a hybrid device geometry, since carrier transport is largely determined by the interface with the semiconductor. For example, even the spin polarization in a heterostructure (which determines the magnitude of magnetoresistive effects) is not uniquely determined by the bulk magnetic material [13]. Structural properties of the interface are important as well: Interfacial defects arising from lattice mismatch between the metal and semiconductor are known to suppress the efficiency with which spin-polarized carriers can be injected into a semiconductor [39]. Even more dramatic changes can result from different choices of the insulating tunnel barrier between two ferromagnetic electrodes: In a recent experiment measuring the tunneling magnetoresistance (TMR) between two CoFe electrodes, replacement of the Al₂O₃ barrier by MgO was shown to increase the room-temperature TMR by 160% (up to 220%) [40], confirming previous theoretical predictions [41, 42]. The choice of tunnel barrier also has a strong influence on transport properties. It was demonstrated that the use of a CoFe/MgO tunnel injector can provide robust room-temperature spin injection in semiconductors such as GaAs [43, 44].

In the second approach to device design (using all-semiconductor structures), a key issue is whether ferromagnetic semiconductors with sufficiently high $T_{\rm C}$ can be developed. While ferromagnetic semiconductors have been known since the studies on CrBr₃ in 1960 [45], a more recent interest in ferromagnetic semiconductors was spurred by the fabrication of (III, Mn)V compounds. After the initial work on (In, Mn)As [46–48], most of the research has focused on (Ga, Mn)As [49–51]. In contrast to (In, Mn)As and (Ga, Mn)As with high carrier density ($\sim 10^{20}$ cm⁻³), a much lower carrier density in (Zn, Cr)Te [52] (a II–VI ferromagnetic semiconductor with $T_{\rm C}$ near room temperature [53]) suggests that transport properties can be effectively controlled by carrier doping.

On the theoretical front, work by Dietl et al. [54, 55] using the Zener model for carrier-mediated ferromagnetism was particularly influential, since it gave predictions of Curie temperatures in a wide range of ferromagnetic semiconductors (**Figure 1**). These findings have stimulated numerous theoretical studies to understand ferromagnetism in semiconductors (some reviewed in [56–61]) and vigorous experimental efforts to fabricate novel ferromagnetic materials. The development of new materials would, of course, be aided significantly by a theoretical understanding of the semiconductor properties that are most important for determining $T_{\rm C}$. At present, this understanding is lacking, even for

idealized homogeneous bulk materials. For example, our first-principles results using density-functional theory reveal a variation of magnetic properties across different materials that cannot be explained by the dominant models of ferromagnetism in semiconductors [62]. Specifically, we considered a single materials family of 64 different Mn-doped II–IV–V₂ chalcopyrites, a ternary generalization of the binary III–V compounds; several have already been reported experimentally to be ferromagnetic [63, 64]. Our results for Mn spin–spin coupling strength J vs. lattice constant a of the host chalcopyrite show no support for the approximate scaling $J \propto a^{-3}$ (or, equivalently, $T_{\rm C} \propto a^{-3}$) that is predicted by the Zener model [54, 55].

Another key issue for all-semiconductor device designs is the external control of $T_{\rm C}$. Dilute magnetic semiconductors offer an intriguing possibility: carriermediated ferromagnetism in materials such as (In, Mn)As, (Ga, Mn)As, and MnGe [65-69], which introduces the possibility of tuning the strength of the ferromagnetic interactions and, therefore, of tuning $T_{\rm C}$. For example, when the number of carriers is changed, either by shining light [70, 71] or by applying a gate bias in a field-effect transistor geometry [72], the material can be switched between the paramagnetic and ferromagnetic states. These experiments suggest the prospect of nonvolatile multifunctional devices with tunable optical, electrical, and magnetic properties. Furthermore, the demonstration of optically or electrically controlled ferromagnetism provides a method for distinguishing carrier-induced semiconductor ferromagnetism from ferromagnetism that originates from metallic magnetic inclusions [73]. Such a distinction is particularly important in view of the growing number of experimental reports of room-temperature ferromagnetism in semiconductors [74]. Indeed, it is difficult to identify spurious sources of magnetism from magnetometry alone. For example, early reports of ferromagnetism at 900 K in La-doped CaBa₆ [75–77] were later revisited and attributed to an extrinsic effect [78].

A high $T_{\rm C}$ value alone is not sufficient for successful integration of ferromagnetic semiconductors in relevant device structures. It is also important to have materials which would have a good lattice match with technologically important nonmagnetic semiconductors. Lattice mismatch typically leads to low-quality interfaces with a high density of interfacial defects, which would be detrimental to spin-polarized transport and effective spin injection. A potentially desirable situation could be realized with II–IV–V₂ chalcopyrites. It can be seen from Figure 2 that the predicted ferromagnetic chalcopyrites span a large lattice constant range. In particular, ZnSiP should be lattice-matched with Si and therefore

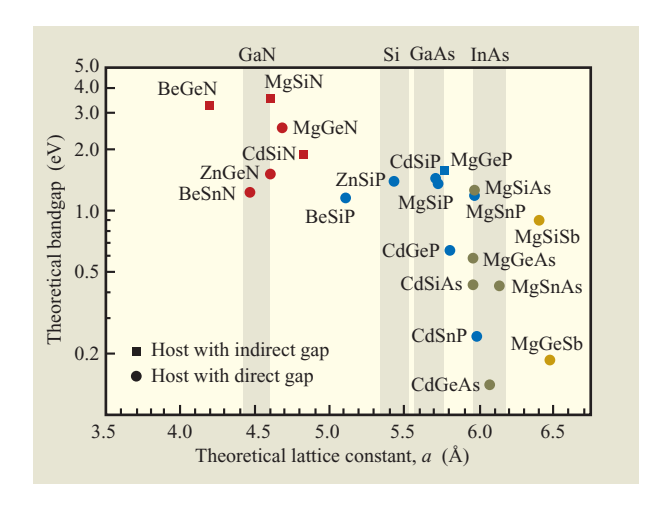


Figure 2

Theoretical bandgap vs. theoretical lattice constant for $II-IV-V_2$ chalcopyrites. Some can be doped with Mn to become ferromagnetic. The shaded areas indicate hosts that are expected to be ($\pm 2\%$) lattice matched to GaN, Si, GaAs, or InAs. The filled symbols denote potentially stable host compounds (negative enthalpies of formation). Adapted from [62], with permission.

might be useful in demonstrating electrical spin injection into silicon [27].

Finally, we note that spintronic devices do not necessarily require the use of ferromagnetic materials or external magnetic fields. The central physical phenomenon—lifting of the spin degeneracy—can also be realized in nonmagnetic materials with the aid of transport, optical, and resonance methods to generate nonequilibrium spin polarization [13]. For example, circularly polarized light provides an effective way to generate net spin polarization in direct-bandgap semiconductors. The angular momentum of the absorbed light is transferred to the medium, leading directly to orientation of the electron orbital momenta and, through spin-orbit interaction, to polarization of the electron spins. In bulk III-V semiconductors such as GaAs, optical orientation can lead to a 50% level of polarization of the electrons; this can be further enhanced by using quantum structures of reduced dimensionality, or by applying strain.

Next, we formulate drift-diffusion equations for bipolar spin-polarized transport and illustrate several of their implications in a nonmagnetic limit, in the absence of equilibrium magnetization. We then consider the magnetic p-n junction and an interplay between equilibrium magnetization and the injected nonequilibrium spin, leading to strong spin-charge coupling. In the last section, we review the basics of

the bipolar junction transistor and our proposal for its generalization—the magnetic bipolar transistor.

Because of space limitations, we illustrate our proposal for bipolar spintronics based only on the above, inevitably omitting many references to the vast field of semiconductor spintronics. Many additional findings and an extensive number of references in semiconductor spintronics have been reviewed in [13].

Bipolar spin-polarized transport

Spin-polarized drift-diffusion equations

We briefly recall here a case of unipolar spin-polarized transport in a metallic regime. We label spin-resolved quantities by $\lambda=1$ or \uparrow for spin-up and $\lambda=-1$ or \downarrow for spin-down along the chosen quantization axis. For a free electron, spin angular momentum and magnetic moment are in opposite directions, and what precisely is denoted by "spin-up" varies in the literature [79]. Conventionally, in metallic systems [80], the term refers to carriers with majority spin. This means that the spin (angular momentum) of such carriers is anti-parallel to the magnetization. Some care is needed with the terminology used for semiconductors, for which the terms *majority* and *minority* refer to the relative population of charge carriers (electrons or holes). Spin-resolved charge current (density) in a diffusive regime can be expressed as

$$j_{i} = \sigma_{i} \nabla \mu_{i} \,, \tag{1}$$

where σ_{λ} is conductivity and the chemical potential (sometimes also referred to as the electrochemical potential) is

$$\mu_{\lambda} = (qD_{\lambda}/\sigma_{\lambda})\delta n_{\lambda} - \phi, \tag{2}$$

with q being the proton charge, D_{λ} the diffusion coefficient, $\delta n_{\lambda} = n_{\lambda} - n_{\lambda 0}$ the change of electron density from the equilibrium value for spin λ , and ϕ the electric potential. We use a notation in which a general quantity X is expressed as the sum of equilibrium and nonequilibrium parts, $X = X_0 + \delta X$. Here we focus on the case of collinear magnetization. More generally, for a non-collinear magnetization, j_{λ} becomes a secondrank tensor [81, 82].

In the steady state, the continuity equation is

$$\nabla j_{\lambda} = \lambda q \left[\frac{\delta n_{\lambda}}{\tau_{\lambda-\lambda}} - \frac{\delta n_{-\lambda}}{\tau_{-\lambda\lambda}} \right], \tag{3}$$

and $\tau_{\lambda\lambda'}$ is the average time for flipping a λ -spin to a λ' -spin. For a degenerate conductor, the Einstein relation is

$$\sigma_1 = q^2 N_1 D_2 \,, \tag{4}$$

where $\sigma = \sigma_{\uparrow} + \sigma_{\downarrow}$ and $N = N_{\uparrow} + N_{\downarrow}$ is the density of states. By using a detailed balance $N_{\uparrow}/\tau_{\uparrow\downarrow} = N_{\downarrow}/\tau_{\downarrow\uparrow}$ [83] together with Equations (2) and (4), the continuity equation can be expressed [84, 85] as

$$\nabla j_{\lambda} = \lambda q^2 \frac{N_{\uparrow} N_{\downarrow}}{N_{\uparrow} + N_{\downarrow}} \frac{\mu_{\lambda} - \mu_{-\lambda}}{\tau_{s}} , \qquad (5)$$

where $\tau_s = \tau_{\uparrow\downarrow}\tau_{\downarrow\uparrow}/(\tau_{\uparrow\downarrow} + \tau_{\downarrow\uparrow})$ is the spin relaxation time. Equation (5) implies the conservation of charge current $j=j_{\uparrow}+j_{\downarrow}=$ constant, while the spin counterpart, the difference of the spin-polarized currents $j_s=j_{\uparrow}-j_{\downarrow}$, is position-dependent.

Spin-polarized bipolar transport can be thought of as a generalization of its unipolar counterpart. Specifically, spin-polarized unipolar transport, in a metallic regime, can then be obtained as a limiting case by setting the electron-hole recombination rate to zero and considering only one type of carrier (either electrons or holes). In the absence of any spin polarization, equations that aim to describe spin-polarized bipolar transport must recover a description of charge transport. Conventional charge transport in semiconductors is often accompanied by large deviations from local charge neutrality (for example, due to materials inhomogeneities, interfaces, and surfaces), and Poisson's equation must be explicitly included in an analysis of such transport. If we consider (generally inhomogeneous) doping with a density of N_a ionized acceptors and $N_{\rm d}$ donors, we can write

$$\nabla \cdot (\epsilon \nabla \phi) = q(n - p + N_a - N_d), \tag{6}$$

where n and p (electron and hole densities) also depend on the electrostatic potential ϕ and permittivity ϵ , and can be spatially dependent. In contrast to the metallic regime, even equilibrium carrier density can have large spatial variations that can be routinely tailored by an appropriate choice of the doping profile $[N_{\rm d}(x)-N_{\rm a}(x)]$. Furthermore, charge transport in semiconductors can display strong nonlinearities, for example, as in the exponential-like current–voltage dependence of a diode [30].

Returning to the case of spin-polarized transport in semiconductors, we formulate a drift-diffusion model which generalizes the considerations of Equations (1)–(5) to include both electrons and holes [24, 25, 86]. We recall from Equations (1) and (2) that spin-resolved current has a drift part (proportional to the electric field; i.e., $\propto \nabla \phi$) and a diffusive part ($\propto \nabla n_{\lambda}$), which we extend to capture the effects of band bending, band offsets, various materials inhomogeneities, and the presence of two types of charge carriers.

To introduce our notation and terminology, which is a direct generalization of what is conventionally used in semiconductor physics [87], we first consider the expression for quasi-equilibrium carrier densities. For nondegenerate doping levels (Boltzmann statistics) the spin-resolved components are

$$n_{\lambda} = \frac{N_{\rm c}}{2} e^{-[E_{\rm c\lambda} - \mu_{\rm n,l}]/k_{\rm B}T}, \quad p_{\lambda} = \frac{N_{\rm v}}{2} e^{-[\mu_{\rm p\lambda} - E_{\rm v,l}]/k_{\rm B}T}, \tag{7}$$

where subscripts c and v label quantities which pertain to the conduction and valence bands. For example, $N_{\rm c,v}=2(2\pi m_{\rm c,v}^*k_{\rm B}T/h^2)^{3/2}$ represent the effective density of states with the corresponding effective masses $m_{\rm c,v}^*$, and $k_{\rm B}$ is the Boltzmann constant. From the total electron density $n=n_{\uparrow}+n_{\downarrow}$ and the spin density $s=n_{\uparrow}-n_{\downarrow}$, we can define the spin polarization of electron density as

$$P_{\rm n} = \frac{s}{n} = \frac{n_{\uparrow} - n_{\downarrow}}{n_{\uparrow} + n_{\downarrow}} \,. \tag{8}$$

We consider a general case in which the spin-splitting of conduction and valence bands, expressed respectively as $2q\zeta_c$ and $2q\zeta_v$, can be spatially inhomogeneous [25]. Splitting of carrier bands (Zeeman or exchange) can arise because of doping with magnetic impurities and/or the presence of an applied magnetic field. The spin- λ conduction band edge (**Figure 3**),

$$E_{c\lambda} = E_{c0} - q\phi - \lambda q\zeta_c, \qquad (9)$$

differs from the corresponding nonmagnetic bulk value E_{c0} because of the electrostatic potential ϕ and spinsplitting $\lambda q\zeta_c$. The discontinuity of the conduction band edge is denoted by ΔE_c . In the nonequilibrium state, the chemical potential for the λ -electrons is $\mu_{n\lambda}$ and generally differs from the corresponding quantity for the holes. While $\mu_{n\lambda}$ is analogous to the electrochemical potential in Equations (1) and (2), following the conventional semiconductor terminology, we refer to it here as the chemical potential, which is also known as the quasi-Fermi level. An analogous notation holds for the holes and the valence band. For example, in Equation (7) p_{λ} is the spin- λ density of the holes, with $E_{v\lambda} = E_{v0} - q\phi - \lambda q\zeta_v$.

By assuming drift-diffusion-dominated transport across the heterojunction, the spin-resolved chargecurrent densities can be expressed [27] as

$$\mathbf{j}_{\mathrm{n}\lambda} = \overline{\mu}_{\mathrm{n}\lambda} n_{\lambda} \nabla E_{\mathrm{c}\lambda} + q D_{\mathrm{n}\lambda} N_{\mathrm{c}} \nabla (n_{\lambda}/N_{\mathrm{c}}) \,, \tag{10}$$

$$\mathbf{j}_{\mathbf{p}\lambda} = \overline{\mu}_{\mathbf{p}\lambda} p_{\lambda} \nabla E_{\mathbf{v}\lambda} - q D_{\mathbf{p}\lambda} N_{\mathbf{v}} \nabla (p_{\lambda}/N_{\mathbf{v}}) , \qquad (11)$$

where $\overline{\mu}$ and D are mobility and diffusion coefficients (we use the symbol $\overline{\mu}$ to distinguish it from the chemical potential μ). In nondegenerate semiconductors, $\overline{\mu}$ and D are related by the Einstein relation

$$\overline{\mu}_{\mathbf{n},\mathbf{n}\lambda} = qD_{\mathbf{n},\mathbf{n}\lambda}/k_{\mathbf{B}}T,\tag{12}$$

which differs from the metallic (completely degenerate) case given by Equation (4).

With two types of carriers, the continuity equations are more complex than those for metallic systems.

After including additional terms for the recombination of electrons and holes as well as the photoexcitation

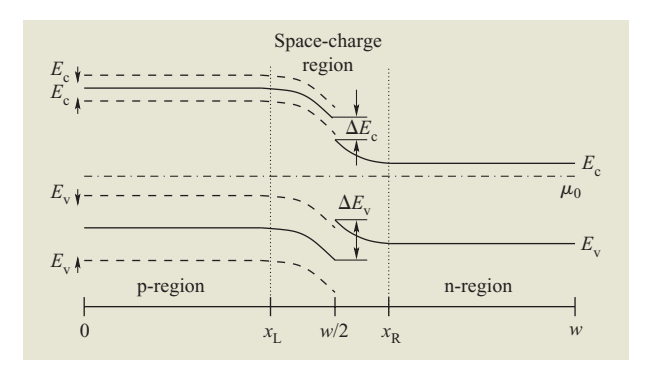


Figure 3

Band diagram for hypothetical magnetic heterojunction. In equilibrium, the chemical potential μ_0 is constant. Conductance and valence-band edges $(E_{\rm c}$ and $E_{\rm v})$ are spin-split in the magnetic pregion, while in the nonmagnetic n-region there is no spin splitting. The left and right edges of a space-charge (depletion) region are denoted by $x_{\rm L}$ and $x_{\rm R}$. For a sharp doping profile, at x=w/2, there are generally discontinuities in the conduction and valence bands $(\Delta E_{\rm c}$ and $\Delta E_{\rm v})$ and in other quantities such as the effective mass, permittivity, and diffusion coefficient.

of electron-hole pairs, we can write these equations as

$$\begin{split} -\frac{\partial n_{\lambda}}{\partial t} + \nabla \cdot \frac{\mathbf{j}_{\mathbf{n}\lambda}}{q} &= + r_{\lambda} (n_{\lambda} p_{\lambda} - n_{\lambda 0} p_{\lambda 0}) \\ &+ \frac{n_{\lambda} - n_{-\lambda} - \lambda \tilde{s}_{\mathbf{n}}}{2\tau_{\mathbf{sn}}} - G_{\lambda} \,, \end{split} \tag{13}$$

$$\begin{split} &+\frac{\partial p_{\lambda}}{\partial t} + \nabla \cdot \frac{\mathbf{j}_{\mathbf{p}\lambda}}{q} = -r_{\lambda}(n_{\lambda}p_{\lambda} - n_{\lambda0}p_{\lambda0}) \\ &-\frac{p_{\lambda} - p_{-\lambda} - \lambda \tilde{s}_{\mathbf{p}}}{2\tau_{\mathbf{p}\mathbf{p}}} + G_{\lambda}. \end{split} \tag{14}$$

The generation and recombination of electrons and holes of spin λ can be characterized by the rate coefficient r_{λ} ; the spin relaxation time for electrons and holes is denoted by $\tau_{\rm sn,p}$; and the photoexcitation rate G_{λ} represents the effects of electron–hole pair generation and optical orientation. Spin relaxation equilibrates carrier spin while preserving nonequilibrium carrier density; for nondegenerate semiconductors $\tilde{s}_{\rm n} = n P_{\rm n0}$, where, from Equation (7), an equilibrium polarization of electron density $P_{\rm n0}$ can be characterized as

$$P_{\rm n0} = \tanh\left(q\zeta_{\rm c}/k_{\rm B}T\right). \tag{15}$$

An analogous expression holds for holes and \tilde{s}_p .

The system of drift-diffusion equations (Poisson and continuity equations) can be self-consistently solved numerically [24, 25, 88], and, under simplifying assumptions (as in the case of charge transport), analytically [27, 86, 89]. Heterojunctions, such as the one

depicted in Figure 3, can be thought of as building blocks of bipolar spintronics. To obtain a self-consistent solution in such a geometry, only the boundary conditions at x=0 and x=w need be specified. On the other hand, to obtain an analytical solution we also need to specify the matching conditions at $x_{\rm L}$ and $x_{\rm R}$, the two edges of the space-charge region (or depletion region), in which there is a large deviation from the local charge neutrality, accompanied by band bending and a strong built-in electric field.

We next illustrate how the matching conditions for spin and carrier density can be applied within the small-bias or low-injection approximation, widely used to obtain analytical results for charge transport [30, 87]. In this case, nonequilibrium carrier densities are small compared with the density of majority carriers in the corresponding semiconductor region. For materials such as GaAs, a small bias approximation gives good agreement with the full self-consistent solution up to approximately 1 V [25, 88].

To simplify our notation, we consider a model for which only electrons are spin-polarized ($p_{\uparrow}=p_{\downarrow}=p/2$), while it is straightforward to also include spin-polarized holes [27, 86]. Outside the depletion charge region, materials parameters (such as $N_{\rm a}$, $N_{\rm d}$, $N_{\rm c}$, $N_{\rm v}$, $\overline{\mu}$, and D) are assumed to be constant. The voltage drop is assumed to be confined to the depletion region, which is highly resistive and depleted from carriers. In thermal equilibrium ($\mu_{\rm n\lambda}=\mu_{\rm p\lambda}=\mu_0$), the built-in voltage $V_{\rm bi}$ can be simply evaluated from Equation (7) as

$$V_{\rm bi} = \phi_{\rm 0R} - \phi_{\rm 0L} \,, \tag{16}$$

while the applied bias V (taken to be positive for forward bias) can be expressed as

$$V = -(\delta\phi_{\rm R} - \delta\phi_{\rm I}),\tag{17}$$

implying that the total junction potential between x = 0 and x = w is $V - V_{\rm bi}$. For the heterojunction of Figure 3, the width of the depletion (space-charge) region is

$$x_{\rm R} - x_{\rm L} \propto \sqrt{V_{\rm bi} - V},\tag{18}$$

where the built-in voltage is represented by $qV_{\rm bi} = -\Delta E_{\rm c} + k_{\rm B}T \ln (n_{\rm 0R}N_{\rm cR}/n_{\rm 0L}N_{\rm cL})$. Outside the depletion region, the system of drift-diffusion equations reduces to only diffusion equations for spin density and the density of minority carriers, while the density of majority carriers is simply given by the density of donors and acceptors [25, 86].

From Equation (7) we rewrite the electron density by separating various quantities into equilibrium and nonequilibrium parts:

$$n_{\lambda} = n_{\lambda 0} \exp\left[(q\delta\phi + \delta\mu_{\rm n}\lambda)/k_{\rm B}T\right]. \tag{19}$$

The electron carrier and spin density (for simplicity we omit the subscript n when writing $s = n_{\uparrow} - n_{\downarrow}$) can be expressed [86] as

$$n = e^{(\delta\phi + \delta\mu_+)/k_{\rm B}T)} \left[n_0 \cosh \left(\frac{q\mu_-}{k_{\rm B}T} \right) + s_0 \sinh \left(\frac{q\mu_-}{k_{\rm B}T} \right) \right], \quad (20)$$

$$s = e^{(\delta\phi + \delta\mu_+)/k_{\rm B}T)} \left[n_0 \sinh\left(\frac{q\mu_-}{k_{\rm B}T}\right) + s_0 \cosh\left(\frac{q\mu_-}{k_{\rm B}T}\right) \right], \quad (21)$$

where $\mu_{\pm} \equiv (\mu_{n\uparrow} \pm \mu_{n\downarrow})/2$, and the polarization of electron density is

$$P_{\rm n} = \frac{\tanh{(q\mu_{-}/k_{\rm B}T)} + P_{\rm n0}}{1 + P_{\rm n0}\tanh{(q\mu_{-}/k_{\rm B}T)}} \,. \tag{22}$$

If we assume that the spin-resolved chemical potentials are constant for $x_L \le x \le x_R$ (i.e., that the depletion region is sufficiently narrow that the spin relaxation and carrier recombination can be neglected in the region), it follows, from Equation (22) and $\tan h (q_{\mu_-}/k_B T) \equiv constant$, that

$$P_{\rm n}^{\rm L} = \frac{P_{\rm n0}^{\rm L} [1 - (P_{\rm n0}^{\rm R})^2] + \delta P_{\rm n}^{\rm R} (1 - P_{\rm n0}^{\rm L} P_{\rm n0}^{\rm R})}{1 - (P_{\rm n0}^{\rm R})^2 + \delta P_{\rm n}^{\rm R} (P_{\rm n0}^{\rm L} - P_{\rm n0}^{\rm R})},$$
(23)

where L (left) and R (right) label the edges of the space-charge (depletion) region of a p-n junction. Correspondingly, δP_n^R represents the nonequilibrium electron polarization, evaluated at R, arising from a spin source. For a homogeneous equilibrium magnetization $(P_{n0}^L = P_{n0}^R)$, $\delta P_n^L = \delta P_n^R$; the nonequilibrium spin polarization is the same across the depletion region. Equation (23) demonstrates that only *nonequilibrium* spin, already present in the bulk region, can be transferred through the depletion region at small biases [24, 25, 86].

Our assumption of constant spin-resolved chemical potentials is a generalization of a conventional model for charge transport in which both μ_n and μ_p are assumed to be constant across the depletion region [87]. From Equations (17), (20), and (21) we can obtain minority carrier and spin densities at $x = x_L$:

$$n_{\rm L} = n_{0\rm L} e^{qV/k_{\rm B}T} \left[1 + \delta P_{\rm n}^{\rm R} \frac{P_{\rm n0}^{\rm L} - P_{\rm n0}^{\rm R}}{1 - (P_{\rm n0}^{\rm R})^2} \right], \tag{24}$$

$$s_{\rm L} = s_{\rm 0L} e^{qV/k_{\rm B}T} \left[1 + \frac{\delta P_{\rm n}^{\rm R}}{P_{\rm n0}^{\rm L}} \frac{1 - P_{\rm n0}^{\rm L} P_{\rm n0}^{\rm R}}{1 - (P_{\rm n0}^{\rm R})^2} \right], \tag{25}$$

which in the absence of nonequilibrium spin ($\delta P_n^R = 0$) reduce to the well-known Shockley relation for the minority carrier density at the depletion region [29],

$$n_{\rm L} = n_{\rm 0L} e^{qV/k_{\rm B}T},\tag{26}$$

and an analogous formula for the spin,

$$s_{\rm L} = s_{\rm 0L} e^{qV/k_{\rm B}T}. \tag{27}$$

Nonmagnetic limit: Spin-polarized p-n junctions

We apply our previous findings to the nonmagnetic limit of vanishing-equilibrium magnetization or, equivalently, vanishing-equilibrium spin polarization, since $\zeta_c = \zeta_v = 0$. We first consider a homogeneously doped semiconductor in which nonequilibrium spin polarization is created through optical orientation. Holes are assumed to be unpolarized, an accurate approximation in materials such as GaAs; the spin-relaxation time for holes can be several orders of magnitude shorter than the corresponding time for electrons [13, 90]. We can simplify Equations (14) and (15) and consider that holes would recombine with the electrons of either spin. In the steady state, the balance between direct electron–hole recombination and optical pair creation can be obtained from the sum of Equations (13) and (14) for $\lambda = \uparrow$ and \downarrow as

$$r(np - n_0 p_0) = G, (28)$$

where $r=r_{\uparrow}/2=r_{\downarrow}/2$ is the coefficient of the total generation–recombination rate and $G=G_{\uparrow}+G_{\downarrow}$ is the total electron–hole photoexcitation rate. Similarly, from the difference of Equations (13) and (14) for $\lambda=\uparrow$ and \downarrow , the balance between spin relaxation and spin generation can be expressed as

$$rsp + s/\tau_s = P_n(t=0)G, \tag{29}$$

where $P_{\rm n}$ (t=0) is the spin polarization at the moment of photoexcitation, as given by Equation (8). The first term in Equation (29) describes the disappearance of the spin density because of carrier recombination, while the second term describes the intrinsic spin relaxation. From Equations (28) and (29) we obtain the steady-state electron polarization [24],

$$P_{\rm n} = P_{\rm n}(t=0) \frac{1 - n_0 p_0 / np}{1 + 1/\tau_{\rm s} rp} \ . \eqno(30)$$

In a p-doped sample, $p \approx p_0$, $n \gg n_0$, and Equation (30) gives

$$P_{\rm n} = P_{\rm n}(t=0)/(1+\tau_{\rm n}/\tau_{\rm s}),\tag{31}$$

where $\tau_{\rm n}=1/rp_0$ is the electron lifetime. After the illumination is switched off, the electron spin density, or, equivalently, the nonequilibrium magnetization, decreases exponentially with the inverse time constant [91]:

$$1/T_{s} = 1/\tau_{p} + 1/\tau_{s}. \tag{32}$$

The steady-state polarization is independent of the illumination intensity, being reduced from the initial spin polarization $P_n(t=0)$. The polarization of the photoluminescence is $P_{circ} = P_n(t=0)P_n$ [91].

For spin pumping in an n-doped sample, where $n \approx n_0$ and $p \gg p_0$, Equations (28) and (30) give [92]

$$P_{\rm p} = P_{\rm p}(t=0)/(1 + n_0/G\tau_{\rm s}). \tag{33}$$

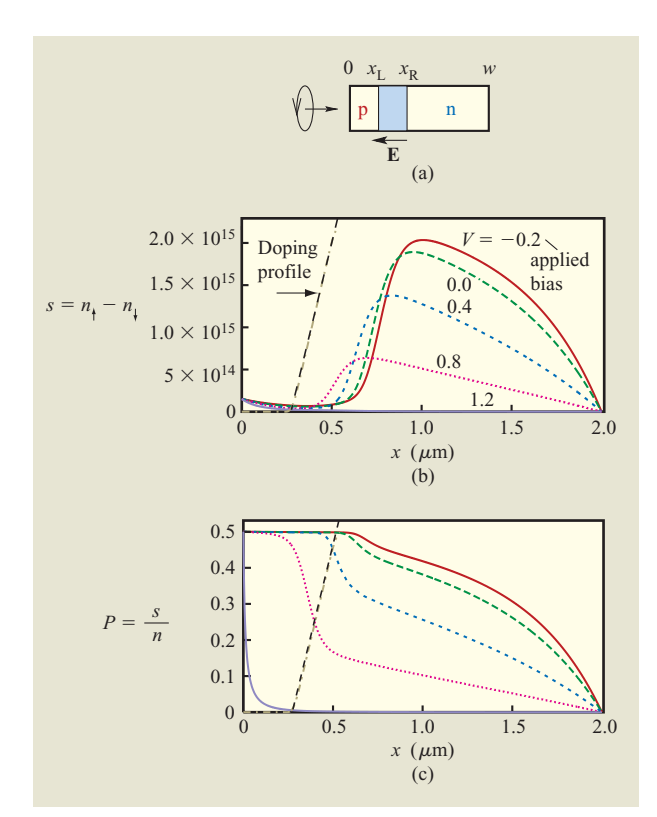
In contrast to the previous case, the hole lifetime $\tau_{\rm p}=1/rn_0$ has no effect on $P_{\rm n}$. However, $P_{\rm n}$ depends on the photoexcitation intensity G, as expected for a pumping process. The effective carrier lifetime is $\tau_J=n_0/G$, where J represents the intensity of the illuminating light. If it is comparable to or shorter than $\tau_{\rm s}$, spin pumping should be very effective. Spin pumping should occur because the photoexcited spin-polarized electrons should not need to recombine with holes. There would be a sufficient supply of unpolarized electrons in the conduction band available for recombination. The spin would thus be pumped into the electron system.

From the previous results for optical illumination in homogeneously doped p- and n-regions, one can obtain spin and charge diffusion lengths via the expression

$$L = \sqrt{D\tau},\tag{34}$$

in which L would provide a characteristic length scale for the spatial decay of nonequilibrium spin or charge by substituting for D the appropriate (electron or hole) diffusion coefficient and for τ (spin or charge) the characteristic time scale. Early experiments using optical orientation have provided a direct measurement of the characteristic time scale for the decay of the nonequilibrium spin [31]. More recent important optical measurements have shown that such a time scale—the spin lifetime in GaAs—can be enhanced by an order of magnitude [93] (>40 ns) or even by two orders of magnitude [94, 95] (>100 ns). The related issues of spin relaxation and spin dephasing in GaAs have been extensively reviewed in [13].

We next discuss our proposal for spin-polarized p-n junctions, which can be viewed as a generalization of optical orientation in homogeneously doped semiconductors, and discuss several novel effects. A particular realization of a spin-polarized p-n junction, illustrated in Figure 4(a), would combine two key ingredients: 1) nonequilibrium spin produced by optical orientation and 2) a built-in field which separates electron-hole pairs created by illumination. Our choice of numerical parameters is based on the assumed use of a 2-µm-long GaAs sample at room temperature, doped with $N_a = 3 \times 10^{15} \text{ cm}^{-3}$ acceptors on the left and with $N_{\rm d} = 5 \times 10^{15} \, {\rm cm}^{-3}$ donors on the right [the doping profile, $N_{\rm d}(x) - N_{\rm a}(x)$, is shown in **Figure 4(b)**]. The intrinsic carrier concentration is $n_i = 1.8 \times 10^6 \text{ cm}^{-3}$. For an undoped semiconductor, $n_0 = p_0 = n_i$, where n_i can be expressed from Equation (7) as $n_i^2 = N_c N_v \exp(-E_g/k_B T)$. The electron (hole) mobility and diffusion coefficients



Scheme of a spin-polarized p-n junction and associated spin capacitance effect. (a) Schematic representation of the junction, a shaded region (between $x_{\rm L}$ and $x_{\rm R}$) depicts a depletion region with the built-in field **E**. Illumination by circularly polarized light from the left (at x=0) creates electron-hole pairs and orients the spins of the electrons, which diffuse toward the depletion region where they are swept by the field **E** to the n-region. (b) and (c) Bias-dependent spatial profiles of electron spin density and the corresponding spin polarization, showing that the accumulated nonequilibrium spin changes as a function of applied bias; we refer to this as the spin capacitance effect. Adapted from [24], with permission; ©2001 American Physical Society.

are 4,000 (400) cm²·V⁻¹·s⁻¹ and 103.6 (10.36) cm²·s⁻¹. The total recombination rate is assumed to be $r = (1/3) \times 10^{-5}$ cm³·s⁻¹, giving an electron lifetime in the p-region of $\tau_{\rm n} = 1/rN_{\rm a} = 0.1$ ns, and a hole lifetime in the n-region of $\tau_{\rm p} = 1/rN_{\rm d} = 0.06$ ns. The spin relaxation time (which is the spin lifetime in the n-region) is calculated to be $\tau_{\rm s} = 0.2$ ns. In the p-region, the electron spin decays on a time scale of [recall Equation (32)] $T_{\rm s} = \tau_{\rm s} \tau_{\rm n}/(\tau_{\rm s} + \tau_{\rm n}) \approx 0.067$ ns. The minority diffusion lengths are $L_{\rm n} = \sqrt{D_{\rm n}\tau_{\rm n}} \approx 1~\mu{\rm m}$ for electrons in the p-region, and $L_{\rm p} = \sqrt{D_{\rm p}\tau_{\rm p}} \approx 0.25~{\rm for}$ holes in the n-region. The spin decays on the length scale of $L_{\rm sp} = \sqrt{D_{\rm n}T_{\rm s}} \approx 0.8~\mu{\rm m}$ in the p-region and $L_{\rm sn} = \sqrt{D_{\rm n}\tau_{\rm s}} \approx 1.4~\mu{\rm m}$ in the n-region.

Circularly polarized light is assumed to be incident at the left end (x = 0), while ohmic boundary conditions are imposed at the right end (spin density is set to vanish at $x = w = 2 \mu m$). In a metallic regime, away from the point of spin injection (at an interface with a magnetic region), there is usually a monotonic spatial decay of spin density in the nonmagnetic region [13]. However, the spin density in Figure 4(b) shows a qualitatively different, nonmonotonic, behavior. Away from the point of spin injection (x = 0), there is an increase of spin density inside the nonmagnetic region. We refer to this effect as a (spatial) spin density amplification [24]; it is one of the predictions for a spin-polarized p-n junction having inhomogeneous doping. Similar behavior was also predicted via subsequent calculations [96]. An efficient transfer of spin across a ZnSe/GaAs heterojunction [97] suggests that a spatial amplification of spin density could be realized in more general geometries, and not just in p-n junctions.

Figure 4(b) and Figure 4(c) indicate that the spin density and the corresponding spin polarization can vary strongly with bias. As in the case of conventional p-n junctions, with an application of forward (positive) bias, the width of the depletion region decreases [recall Equation (18)]. Since in all of the cases of Figure 4 illumination is assumed to be at x = 0, $P_{\rm I}^{\rm n}$ is reduced for V > 0. At forward bias, x_L (an effective length of the p-region) increases, and electrons must travel farther and experience additional spin decay before being swept (by the built-in field) into the n-region. By analogy with junction capacitance, we designate this as the spincapacitance effect [24], reflecting that an accumulated spin is bias-dependent (a spin capacitance was also recently predicted in the rather different geometry of a field-effect transistor [98]). Another interesting property of a spinpolarized p-n junction would be that it could be a source of spin electromotive force (EMF) to generate spinpolarized currents at no applied bias and to provide an open circuit voltage [88]. In addition to our proposal for a p-n junction-based spin-polarized solar battery [88], a wide range of other structures have recently been suggested as a source of spin EMF [99-101]; these are often referred to as spin(-polarized) pumps, cells, or batteries.

Magnetic p-n junctions

Including spin polarization in p-n junctions could lead to effects such spin capacitance, spin amplification, and the generation of spin EMF, as discussed in the previous section. However, in the absence of equilibrium magnetization and for the geometry of Figure 4(a), there should not be strong coupling between spin and charge. Changing the helicity of the illuminating light implies that

 $P_{\rm n} \rightarrow -P_{\rm n}$ or $s \rightarrow -s$, but the charge properties such as the charge current or open-circuit voltage would remain the same. In this section we discuss how the presence of equilibrium magnetization or, equivalently, equilibrium spin polarization might lead to strong spin-charge coupling. In particular, changing an injected nonequilibrium spin could produce measurable effects on charge properties.

For potential spintronic applications [13], as well as to demonstrate novel effects due to spin-polarized bipolar transport, it is desirable to have large carrier spinsub-band splitting (see Figure 3). In the absence of magnetic field, such a splitting can be achieved by using ferromagnetic semiconductors, while in the presence of such a field one could utilize large effective g-factors due either to magnetic impurities [102] or to spin-orbit coupling in narrow-bandgap semiconductors. For example, in (Cd, Mn)Se, $|g| \approx 500$ at T < 1 K [103]; in n-doped (In, Mn)As, |g| > 100 at 30 K [104]; and in a narrow-bandgap InSb, $|g| \approx 50$ even at room temperature. Selective doping with magnetic impurities and/or an application of an inhomogeneous magnetic field could be used to realize a desirable, spatially inhomogeneous spin-splitting. Inhomogeneous spinsplitting can also occur in domain walls (see for example [105]). By solving a system of drift-diffusion and Poisson equations, one can show that an inhomogeneous spinsplitting leads to deviations from local charge neutrality

We discuss several properties of magnetic p-n junctions that rely on the interplay of the carrier spin-sub-band splitting (implying that there is a finite equilibrium spin polarization of carrier density) and the nonequilibrium spin induced for example by optical or electrical means. We also focus here on a diffusive regime, while a magnetic diode in a ballistic regime was recently discussed in [106]. For simplicity, we examine a particular case in which the band-offsets (see for example Figure 3) are negligible, the spin polarization of holes can be neglected, and in the notation for both the carrier spin-splitting $2q\zeta$ and the spin density s we can omit the index n. A simple schematic of such a magnetic p-n junction is shown in **Figure 5**.

From Equations (7) and (9) we can rewrite the product of equilibrium densities as

$$n_0 p_0 = n_i^2 \cosh{(q\zeta/k_{\rm B}T)}, \tag{35} \label{eq:35}$$

where n_i is the intrinsic (nonmagnetic) carrier density [87]. Note that the density of minority carriers in the p-region should depend on the spin-splitting $n_0(\zeta) = n_0(\zeta = 0) \cosh{(q\zeta/k_BT)}$. As in the theory of charge transport in nonmagnetic junctions [29], the total charge current can be expressed as the sum of minority carrier currents at the deletion edges $j = j_{\rm nL} + j_{\rm pR}$, with

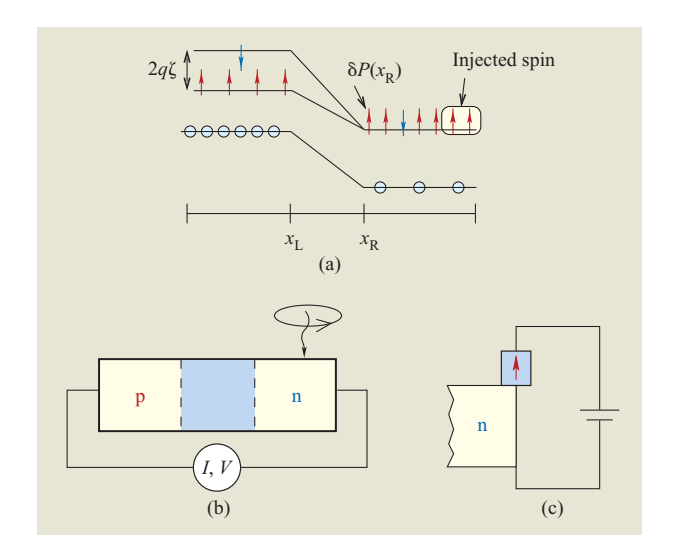
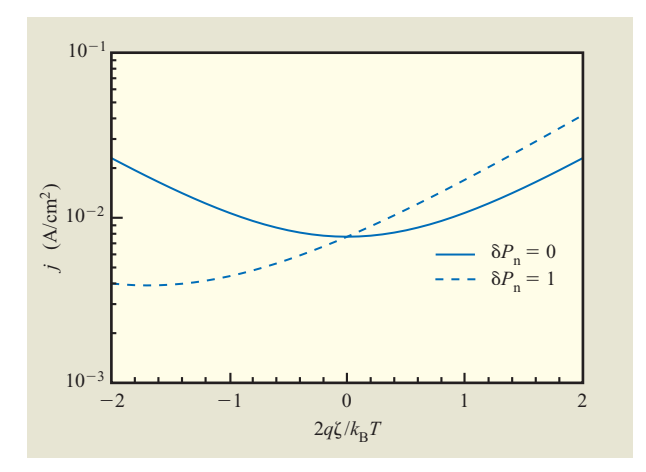


Figure 5

Potential magnetic p—n junction. (a) Band-energy diagram with spin-polarized electrons (arrows) and unpolarized holes (circles), showing the spin-splitting $2q\zeta$, the nonequilibrium spin polarization at the depletion region edge $\delta P_{\rm n}(x_{\rm R})$, and the region where the spin is injected. (b) Junction schematic. Using circularly polarized light (photoexcited electron—hole pairs absorb the angular momentum carried by the incident photons), nonequilibrium spin is injected transversely into the nonmagnetic n-region. The circuit loop for obtaining I-V characteristics is indicated. (c) An alternative scheme to electrically inject spin into the n-region. Adapted from [89], with permission.

$$j_{\rm nL} \propto \delta n_{\rm L} \,, \quad j_{\rm pR} \propto \delta p_{\rm R} \,, \tag{36}$$

where $\delta n_{\rm L}$ is given by Equation (24), with $P_{\rm n0}^{\rm R}=0$, $\delta p_{\rm R} = p_0 [\exp(qV/k_{\rm B}T) - 1]$, and V the applied bias (positive for forward bias). Equation (35) implies that in the regime of large spin-splitting, $q\zeta > k_BT$, the density of minority electrons changes exponentially with $B (\propto \zeta)$ and could create exponentially large magnetoresistance [25]. In the absence of an external spin source, a geometry depicted in Figures 5(a) and 5(b) can also be used to illustrate the prediction of spin extraction [25], a process opposite to spin injection. Spin-splitting in the p-region should provide spin-dependent barriers for electron transport across the depletion region. With a large forward-applied bias and the generation of nonequilibrium carrier density, there could be a significant spin extraction from the nonmagnetic n-region into the magnetic p-region, with spin densities having opposite signs in these two regions (for $s_{0L} > 0$ there would be a spin accumulation $\delta s_{\rm R} < 0$). These findings, obtained from a self-consistent numerical solution of drift-diffusion equations [25], can also be confirmed analytically within the small bias approximation [86]. Similar spin extraction was recently observed



Calculated giant-magnetoresistance (GMR) effect in magnetic diodes. Current/spin-splitting characteristic ($I-\zeta$) are calculated self- consistently at $V=0.8~\rm V$ for the diode of Figure 5. Spin-splitting $2q\zeta$ in the p-region is normalized to $k_{\rm B}T$. The solid curve corresponds to a switched-off spin source. The current is symmetric in ζ . With the spin source on (the extreme case 100% spin polarization injected into the n-region is shown), the current is a strongly asymmetric function of ζ , displaying large GMR values, as shown by the dashed curve. Materials parameters were assumed to be those of GaAs. Adapted from [25], with permission; ©2002 American Physical Society.

experimentally in MnAs/GaAs junctions [107], and theoretical implications due to tunneling from nonmagnetic semiconductors into metallic ferromagnets were considered [108].

The interplay between the P_{n0} [recall Equation (15)] in the p-region and the nonequilibrium spin source of polarization δP_n in the n-region, at the edge of the depletion region, should determine the I-V characteristics of the diodes. The dependence of the electric current j on $q\zeta$ and δP_n was obtained by both numerical and analytical methods. Numerical calculations [25] were performed by self-consistently solving for the system of drift-diffusion equations, and analytical results [27, 86, 89] were obtained using a small-bias approximation [recall Equations (16)–(27)].

To illustrate the I–V characteristics of potential magnetic p–n junctions, consider the small-bias limit in the configuration of Figure 5. The electron contribution to the total electric current can be expressed from Equations (24) and (36) [25, 87] as

$$j_{\rm nL} \sim n_0(\zeta) \left[e^{qV/k_{\rm B}T} (1 + \delta P_{\rm n} P_{\rm n0}) - 1 \right].$$
 (37)

Equation (37) generalizes the Silsbee–Johnson spincharge coupling [109, 110], originally proposed for ferromagnet/paramagnet metal interfaces, to the case of magnetic p-n junctions. An attractive aspect of the spincharge coupling in p-n junctions, as opposed to metals or degenerate systems, is the nonlinear voltage dependence of the nonequilibrium carrier and spin densities [25, 86], resulting in the exponential enhancement of the effect with increasing V. Equation (37) can be understood qualitatively from Figure 5. In equilibrium ($\delta P_n = 0$ and V = 0), no current flows through the depletion region, since the electron currents from both sides of the junction balance. The balance is disturbed either by applying bias or by selectively populating different spin states, making the flow of one spin species greater than that of the other. In the latter case, the effective barrier associated with the crossing of electrons from the n-side to the p-side is different for spin-up and spin-down electrons (see Figure 5). Current can flow even at V = 0 when $\delta P_n \neq 0$. This is an example of the spin-voltaic effect (a spin analog of the photovoltaic effect), in which nonequilibrium spin causes an EMF [25, 111]. In addition, the direction of the zero-bias current is controlled by the relative sign of P_{n0} and $\delta P_{\rm n}$. In the section on magnetic bipolar transistors, we revisit the implications of spin-voltaic effect in threeterminal structures.

Magnetic p-n junctions should display an interesting giant-magnetoresistance (GMR)-like effect, which follows from Equation (37) [25]. The current should depend strongly on the relative orientation of the nonequilibrium spin and the equilibrium magnetization. Figure 6 plots the current density j, which also includes the contribution from holes, as a function of $2q\zeta/k_BT$ for both the unpolarized ($\delta P_n = 0$) and fully polarized ($\delta P_n = 1$) n-regions. In the first case, j is a symmetric function of ζ , increasing exponentially with increasing ζ because of the increase in the equilibrium minority carrier density $n_0(\zeta)$. In unipolar systems, where transport is due to the majority carriers, such a modulation of the current is not likely, since the majority carrier density is fixed by the density of dopants. A realization of exponential magnetoresistance was recently demonstrated in a very different materials system—that of manganite-titanate heterojunctions [112]—in which an applied magnetic field affected the width of a depletion layer.

If $\delta P_{\rm n} \neq 0$, the current should depend on the sign of $P_{\rm n0} \cdot \delta P_{\rm n}$. For parallel nonequilibrium (in the n-region) and equilibrium spins (in the p-region), most electrons should cross the depletion region through the lower barrier (see Figure 5), increasing the current. In the opposite case of anti-parallel relative orientation, electrons should experience a larger barrier, and the current should be inhibited. This is demonstrated in Figure 6 by the strong asymmetry in j. The corresponding GMR ratio, the difference between j for parallel and antiparallel orientations, can also be calculated analytically from Equation (37) as $2|\delta P_{\rm n} P_{\rm n0}|/(1-|\delta P_{\rm n} P_{\rm n0}|)$ [86].

If, for example, $|Pn_0| = |\delta P_n| = 0.5$, the relative change is calculated to be 66%. The GMR effect should be useful for measuring the spin relaxation rate of bulk semiconductors [89], as well as for detecting nonequilibrium spin in the nonmagnetic region of the p-n junction.

Although practical room-temperature magnetic p-n junctions are yet to be fabricated, and the effects discussed here are currently being experimentally examined¹ [113, 114], magnetic p-n junctions have already been demonstrated. Indeed, Wen et al. [115] were perhaps the first to show that a ferromagnetic p-n junction, based on the ferromagnetic semiconductor CdCr₂Se₄ doped with Ag acceptors and In donors, could act as a diode. Also, photovoltaic diodes have been fabricated using a (Hg, Mn)Te magnetic semiconductor [116]. However, more extensive work on magnetic p-n junctions began after the discovery of (III, Mn)V ferromagnetic semiconductors, discussed in [65]. Heavily doped p-(Ga, Mn)As/n-GaAs junctions have been fabricated [117–121] to demonstrate tunneling interband spin injection. Recently, Tsui et al. [122] have shown that the current in p-CoMnGe/n-Ge magnetic heterojunction diodes can indeed be controlled by a magnetic field.

Further studies of magnetic p-n junctions could also be relevant to a class of bipolar structures known as the spin light-emitting diodes (spin LEDs), now widely used to detect electrically injected spin in semiconductors [123–127]. As in the case of an ordinary LED [30], electrons and holes recombine (in a quantum well or a p-n junction) and produce electroluminescence. However, in a spin LED, as a consequence of radiative recombination of spin-polarized carriers, the emitted light should be circularly polarized and could be used to trace back the degree of polarization of carrier density upon injection into a semiconductor. The spatial separation and spin relaxation between the spin injection and the point of spin detection (in a quantum well) make a fully quantitative analysis of the injected polarization more difficult. It would be valuable to perform realistic calculations of spin-polarized transport and spin injection which would treat the entire spin LED as a single entity [13]. An intriguing possibility for a low-power bipolar spintronic application was recently demonstrated by Rudolph et al. [128] with the operation of a spin laser. The laser was a vertical-cavity surface-emitting laser (VCSEL), optically pumped in the gain medium, consisting of two InGaAs quantum wells, with 50% spin-polarized electrons. The electrons recombine with heavy holes, which are effectively unpolarized, emitting circularly polarized light. The threshold electrical current density, extracted from the pump power for the lasing

operation, was found to be 0.5 A/cm², which is 23% below the threshold current density of the spin-unpolarized VCSEL. Furthermore, for a fixed pump power, the emission power of the laser changed by 400% when the degree of circular polarization of the pump laser was changed. The reason for the decrease in threshold is the selective coupling of spin-polarized electrons to photons with one helicity. While the experiment was conducted at 6 K, room-temperature operation and an electrically pumped counterpart should be viable as well.

Bipolar junction transistor

The proposed magnetic bipolar transistor (MBT) is based on spin population differences relying on ensemble spin (magnetization) and can be viewed as having two magnetic p-n junctions [25, 86] connected in series. MBT builds on the bipolar junction transistor (BJT), a conventional device scheme introduced by Shockley et al. [129] and widely used in signal amplification and processing as well as in fast logic applications. We first introduce BJT and its formalism in order to recall some standard transistor terminology and to make a smooth transition to the magnetic case.

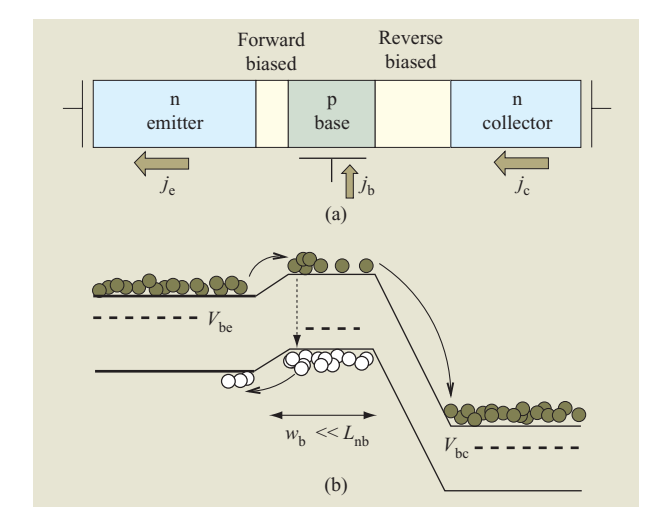
Conventional bipolar junction transistors comprise two p-n junctions in series, forming a three-terminal device. While such an arrangement may sound like a trivial extension of the p-n junction diode, the new structure has the remarkable novel functionality of amplifying small current signals. The structure of an npn BJT is shown in Figure 7. The emitter is doped with N_{de} donors, the base with $N_{\rm ab}$ acceptors, and the collector with $N_{\rm dc}$ donors. The donor (acceptor) densities are also the electron (hole) majority densities in the respective regions. In equilibrium the minority densities are small. For example, the number of conduction electrons in the base is $n_{0b} = n_i^2/N_{ab}$, where n_i is the intrinsic carrier density in the semiconductor. External biases drive the current. In the most useful form of transistor operation, the forward active mode, in which the transistor is an amplifier, the emitter-base junction is forward-biased with a potential $V_{\rm be} > 0$, while the collector-base junction is reverse-biased with a potential $V_{\rm bc} < 0$. Thus, the built-in potential in the emitter-base junction is reduced by V_{be} , permitting electron injection from the emitter to the base. The number of minority electrons in the base close to the junction increases exponentially to the nonequilibrium density

$$n_{\rm be} = n_{0\rm b} e^{qV_{\rm be}/k_{\rm B}T}. (38)$$

As in the section on spin-polarized drift-diffusion equations, we introduce the nonequilibrium (excess) density as

$$\delta n_{\rm be} = n_{\rm be} - n_{\rm 0b} = n_{\rm 0b} (e^{qV_{\rm be}/k_{\rm B}T} - 1).$$
 (39)

¹H. Munekata, Tokyo Institute of Technology, and G. Karczewski, Polish Academy of Sciences, Warsaw, private communications, 2003.



Conventional npn bipolar junction transistor biased in the forward active mode: (a) Overall structure; (b) conduction and valence bands, populated respectively with electrons (filled circles) and holes (empty circles). The dashed lines indicate the Fermi levels (chemical potentials). The emitter–base junction is forward-biased, with potential $V_{\rm bc} > 0$, while the collector–base junction is reverse-biased, with potential $V_{\rm bc} < 0$. The magnitude of the corresponding applied potentials is given by the difference between the Fermi levels. The solid arrows indicate carrier flow, while the dashed arrows illustrate recombination. For effective operation, the base width $w_{\rm b}$ must be less than the electron diffusion length in the base $L_{\rm nb}$.

Similarly, the nonequilibrium electron density in the base at the base–collector junction is

$$\delta n_{\rm bc} = n_{\rm bc} - n_{\rm 0b} = n_{\rm 0b} (e^{qV_{\rm bc}/k_{\rm B}T} - 1). \tag{40}$$

In the forward active mode, $\delta n_{\rm bc}$ is small (and can be neglected) because $V_{\rm bc} < 0$. It becomes important in other modes. The hole excess densities in the emitter and collector, close to the depletion region with the base, are

$$\delta p_{\rm e} = p_{0\rm e} (e^{qV_{\rm be}/k_{\rm B}T} - 1), \qquad (41)$$

$$\delta p_{\rm c} = p_{0\rm c} (e^{qV_{\rm bc}/k_{\rm B}T} - 1) \,. \tag{42} \label{eq:deltap}$$

Again, only $\delta p_{\rm e}$ need be considered in the forward active mode.

The emitter current j_e consists of the electron injection current into the base and the hole injection current into the emitter. As the injected electrons travel through the base, some of them recombine with the holes and leave the base via the valence band. Together with the flow of holes in the opposite direction, this constitutes the hole current j_b . Most of the electrons manage to reach the

collector junction, where they are swept into the collector by the large electric field in the depletion region. Unless recombination occurs inside the depletion region, the electrons reach the collector, forming the collector current j_c together with the holes injected into the collector from the base (this is a small contribution in the forward active mode).

The most interesting characteristic of a transistor is its current gain, defined by

$$\beta = \frac{j_{\rm c}}{j_{\rm h}} \,. \tag{43}$$

Typically $\beta \approx 100$, indicating that a small current signal introduced by varying j_b is amplified a hundred times in the collector circuit. In other words, removal of one electron (per unit time and area) from the base results in the arrival of a hundred electrons at the collector. If there were no current drawn from the base, the electrons recombining there would oppose further injection from the emitter, stopping the current altogether. The sign convention for the current is specified in Figure 7. The base current is

$$j_{\rm h} = j_{\rm e} - j_{\rm c} \,.$$
 (44)

We can calculate β by calculating the currents. A convenient way to write the currents in a BJT is through the nonequilibrium densities of the minority carriers (see for example [130, 131]):

$$j_{\rm e} = j_{\rm gb}^{\rm n} \left[\frac{\delta n_{\rm be}}{n_{\rm ob}} - \frac{1}{\cosh{(w_{\rm b}/L_{\rm nb})}} \frac{\delta n_{\rm bc}}{n_{\rm ob}} \right] + j_{\rm ge}^{\rm p} \frac{\delta p_{\rm eb}}{p_{\rm oe}} \; , \eqno(45)$$

$$j_{\rm c} = j_{\rm gb}^{\rm n} \left[-\frac{\delta n_{\rm bc}}{n_{\rm 0b}} + \frac{1}{\cosh\left(w_{\rm b}/L_{\rm nb}\right)} \frac{\delta n_{\rm be}}{n_{\rm 0b}} \right] - j_{\rm gc}^{\rm p} \frac{\delta p_{\rm cb}}{p_{\rm 0c}} \,. \tag{46}$$

The base current is then calculated using Equation (44). The generation currents j_g reflect the flow of thermally generated carriers in their majority regions close to the depletion region. Such carriers are then swept into the minority sides, regardless of the applied bias. The electron generation current in the base is

$$j_{\rm qb}^{\rm n} = \frac{q D_{\rm nb}}{L_{\rm nb}} n_{\rm 0b} \coth \left(\frac{w_{\rm b}}{L_{\rm nb}}\right). \tag{47} \label{eq:jqb}$$

Here $D_{\rm nb}$ stands for the electron diffusion coefficient in the base whose width is $w_{\rm b}$. As in the case of diodes, the width of a region is an effective (rather than nominal) width, excluding the associated depletion region, whose size depends on the applied bias [recall Equation (18)]. $L_{\rm nb}$ is the electron diffusion length in the base. The hole generation currents in the emitter, $j_{\rm ge}^p$, and collector, $j_{\rm ge}^p$, are

Table 1 Operating modes of conventional and potential magnetic bipolar transistors. Forward (reverse) bias corresponds to positive (negative) voltage *V*. The terms MA and GMA stand for magneto-amplification and giant magneto-amplification, while ON and OFF are modes of small and large resistance, respectively; SPSW designates spin switch. The spin-voltaic mode would apply only to the proposed MBT. From [131], with permission.

Mode	V_{be}	V_{bc}	BJT	MBT
Forward active	Forward	Reverse	Amplification	MA, GMA
Reverse active	Reverse	Forward	Amplification	MA, GMA
Saturation	Forward	Forward	ON	ON, GMA, SPSW
Cutoff	Reverse	Reverse	OFF	OFF
Spin-voltaic	Null	Null	N/A	SPSW

$$j_{\rm ge}^{\rm p} = \frac{qD_{\rm pe}}{L_{\rm pe}} p_{\rm 0e} \coth\left(\frac{w_{\rm e}}{L_{\rm pe}}\right) \,, \tag{48}$$

$$j_{\rm gc}^{\rm p} = \frac{qD_{\rm pc}}{L_{\rm pc}} p_{\rm 0c} \coth\left(\frac{w_{\rm c}}{L_{\rm pc}}\right). \tag{49}$$

The notation is similar to that for the electron case. Equations (39)–(42) and (45)–(49) fully describe the electrical characteristics of ideal bipolar junction transistors. Let us calculate the gain β in the forward active mode. We generalize this calculation for the magnetic case in the next section. The amplification mechanism becomes manifest by introducing three additional quantities: the transport factor α , the base transport factor α_t , and the emitter efficiency γ_e . They are related by

$$\alpha = \alpha_{\rm t} \gamma_{\rm e} = \frac{j_{\rm c}}{j_{\rm e}} \,, \tag{50}$$

where

$$\gamma_{\rm e} = \frac{j_{\rm e}^{\rm n}}{j_{\rm e}},\tag{51}$$

$$\alpha_{\rm t} = \frac{j_{\rm c}}{j_{\rm c}^{\rm n}} \,. \tag{52}$$

The emitter efficiency measures the contribution of electrons to the emitter current. The higher it is, the more electrons (and fewer holes) are injected across the base–emitter junction. The base transport factor α_t shows how many of the injected electrons traverse the base to form the collector current. The current gain is

$$\beta = \frac{\alpha}{1 - \alpha} \,. \tag{53}$$

Ideally, α is close to 1, so that β is large. For efficient current amplification, both efficient emitter injection ($\gamma_e \approx 1$) and base transport are needed.

In the npn BJT, Equations (45) and (46) give for the emitter efficiency

$$\gamma_{\rm e} = \frac{1}{1 + j_{\rm ge}^{\rm p}/j_{\rm gb}^{\rm n}} \,, \tag{54}$$

since $\delta n_{\rm bc}$ and $\delta p_{\rm bc}$ can be neglected in the forward active mode. The base transport factor is

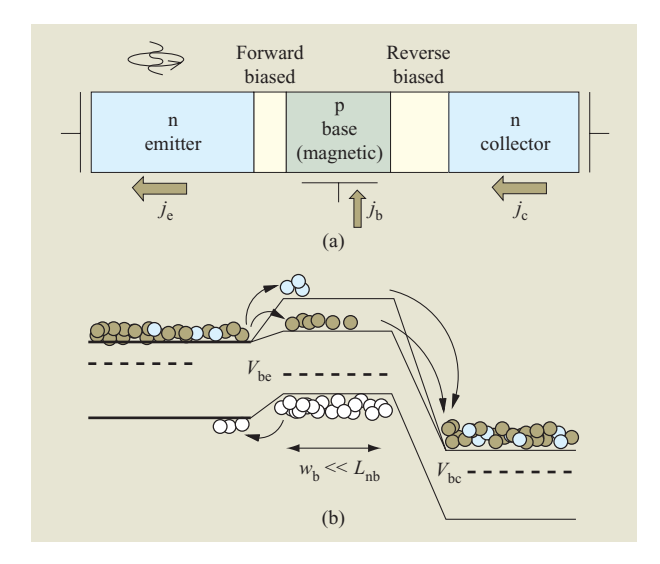
$$\alpha_{\rm t} = \frac{1}{\cosh\left(w_{\rm h}/L_{\rm nb}\right)} \,. \tag{55}$$

The emitter efficiency is usually increased by heavy emitter doping and light base doping, since $j_{\rm ge}^{\rm p}/j_{\rm gb}^{\rm n} \sim N_{\rm ab}/N_{\rm de}$. The greater the doping, the smaller is the equilibrium number of the minority carriers and the corresponding generation current. The base transport factor can be increased by making the base narrower, so that $w_{\rm b} \ll L_{\rm nb}$. In this limit, the transistor amplification factor becomes

$$\beta = \frac{1}{w_b^2 / 2L_{nb}^2 + j_{ge}^p / j_{gb}^n} \,. \tag{56}$$

In Si transistors, it is usually the emitter efficiency that determines amplification, since $L_{\rm nb}$ is rather large in Si because of relatively slow electron–hole recombination. In contrast, GaAs transistors have very small $L_{\rm nb}$ values, and the amplification is limited by the base transport factor. To reduce this factor, spatially modulated GaAs heterostructures are used to create electric drift in the base (to boost the transport).

Table 1 summarizes different operating modes of both conventional BJT and potential magnetic transistors (the latter are discussed in the next section). We have described the active forward mode, in which a BJT amplifies small signals. The reverse active mode simply reverses the biases. In this mode, a BJT can also amplify signals, but β is much smaller because the emitter efficiency is small. Usually transistors have a small



Proposed magnetic npn bipolar transistor in the forward active mode: (a) Overall structure; (b) corresponding bands and bandgap. The notation is as in Figure 7. Only the base has an equilibrium electron spin polarization $P_{0\rm b}$, illustrated in part (b) by the spin-split conduction band. Spin up (down) electrons are shown as dark (light) filled circles. Holes are unpolarized. The emitter is assumed to have a source of spin polarization, here shown as circularly polarized incident light giving rise to nonequilibrium spin polarization δP_e . The coupling between the equilibrium and nonequilibrium polarizations is expected to give rise to many new functionalities, as described in the text. From [131], with permission.

collector doping in order to have large breakdown voltage in the reverse mode. In the saturation mode, both junctions are forward biased. The collector and base currents are similar in magnitude, and amplification is inhibited. This mode, used in logic circuits, is denoted as ON, in contrast to the high-resistance cutoff (OFF) state, in which both junctions are reverse biased and only small currents of the magnitudes of the generation current flow. More discussion can be found in standard textbooks; see for example [132].

Magnetic bipolar transistor

The magnetic bipolar transistor (MBT) was initially proposed as a bipolar junction transistor that would contain magnetic semiconductors as its active elements [26, 133]. Such a transistor is depicted in **Figure 8**. Simplified variations of the MBT, not including the effects of nonequilibrium spin, were later considered by Lebedeva and Kuivalainen [134], by Flatté et al. [135], and by Bandyopadhyay and Cahay [136]. Experimental realization of GaAs/(Ga, Mn)As-based MBT is currently in progress.² The magnetic semiconductors can be

²M. Field, Rockwell Scientific, Thousand Oaks, CA, private communication, 2004.

ferromagnetic or they can have giant g factors and be placed in a magnetic field. Whatever the case, there is a large (comparable to thermal energy), spin-splitting $2q\zeta_b$ of the carrier bands. Here we illustrate the predicted properties of MBTs using electron spin polarization (assuming that the holes are unpolarized). Only the base will have equilibrium spin polarization. Exciting new features appear when we allow for a nonequilibrium spin to be added (which can viewed as a generalization of a simplified scheme that considers only the effects of equilibrium spin [134, 135]. This should be achievable by optical spin orientation or electrical spin injection.

We assume that there is a nonequilibrium spin of polarization $\delta P_{\rm e}$ in the emitter and the equilibrium spin of polarization $P_{\rm 0b}$ in the base. The presence of a magnetic field can modify $P_{\rm 0b}$ by changing $q\zeta_{\rm b}$, since [recall Equation (15)] $P_{\rm 0b} = \tanh{(q\zeta_{\rm b}/k_{\rm B}T)}$.

The most important new feature of the MBT is the spin-dependent barrier for electron injection from the emitter to the base. As indicated in Figure 7, this barrier favors spin-up electrons. More electrons would thus be injected into the lower conduction level in the base than into the upper conduction level. The equilibrium spin polarization in the base would be preserved. We have learned in the previous section that emitter efficiency γ_e is a limiting factor in amplification. We should be able to modify γ_e in the MBT by increasing or decreasing the spin-up electrons in the emitter so that more (fewer) electrons would be injected through the lower spin barrier. It should be possible to achieve this by introducing nonequilibrium spin $\delta P_{\rm e}$. In effect, the emitter efficiency could thus be controlled by spin-charge coupling. As for the base transport factor α_t , there is not much to be done by either spin or magnetic field. While this factor is governed by electron diffusion, there is a possibility that L_{nb} depends on the applied magnetic field, leading to small magnetic effects (also observed for conventional transistors).

The electrical currents through MBTs should also depend on the nonequilibrium minority carrier densities and on the applied biases. The expressions for the currents were given in the previous section [Equations (45) and (46)]. The difference now is that the nonequilibrium electron densities would depend on spin. The spin-charge coupling should lead to the familiar $\delta P_{\rm e} P_{\rm 0b}$ dependence for the electron densities,

$$\delta n_{\rm be} = n_{0\rm b}(\zeta_{\rm b}) \left[e^{qV_{\rm be}/k_{\rm B}T} (1 + \delta P_{\rm e} P_{0\rm b}) - 1 \right], \eqno(57)$$

$$\delta n_{\rm bc} = n_{0\rm b}(\zeta_{\rm b}) \left(e^{qV_{\rm bc}/k_{\rm B}T} - 1 \right). \tag{58}$$

The influence of the equilibrium spin appears both in n_{0b} (ζ_b) = $n_{0b}(0) \cosh{(q\zeta_b/k_BT)}$, which reflects the change of the equilibrium minority density in the magnetic region, and in the spin-charge coupling factor. The nonequilibrium spin plays a role only in the latter.

The expression for $\delta n_{\rm bc}$ remains Equation (40). The excess hole densities are given by Equations (41) and (42).

Substituting δn_{be} from Equation (57) into the formula for j_e [Equation (45)], we obtain for the emitter efficiency

$$\gamma_{\rm e} = \left[1 + \frac{j_{\rm ge}^{p}}{j_{\rm gb}^{n}(\zeta_{\rm b})} \frac{1}{1 + \delta P_{\rm e} P_{\rm 0b}} \right]^{-1}.$$
 (59)

This generalizes Equation (54) to the case of equilibrium spin polarization in the base and the presence of spin-charge coupling. We specify that $j_{\rm gb}^{\rm n}$ depends on $\zeta_{\rm b}$ through $n_{\rm 0b}$ ($\zeta_{\rm b}$). The base factor $\alpha_{\rm t}$ is given by Equation (55). The gain β is then

$$\beta = \left[\frac{w_{\rm b}^2}{2L_{\rm nb}^2} + \frac{j_{\rm ge}^p}{j_{\rm nb}^n(\zeta_{\rm b})} \frac{1}{1 + \delta P_{\rm e} P_{\rm 0b}} \right]^{-1},\tag{60}$$

where we assume the narrow base limit $w_b \ll L_{\rm nb}$. The above formula generalizes Equation (56). The amplification depends on both the equilibrium and nonequilibrium spin. The dependence on the equilibrium spin is through both $j_{\rm gb}^{\rm n}(\zeta_{\rm b})$, which is an even function of $\zeta_{\rm b}$, and thus also $P_{0\rm b}$, and through spin-charge coupling. We designate this dependence as magneto-amplification (MA), since it allows a control over amplification by a magnetic field, giving rise to the equilibrium spin polarization. Magneto-amplification should be present even without the nonequilibrium spin and should be useful for detecting a magnetic field or for measuring the equilibrium spin polarization. In analogy with giant magnetoresistance, we designate the effect of a relative change of β upon switching the sign of $\delta P_{\rm e} P_{0\rm b}$ as giant magneto-amplification (GMA) [130, 131]. The corresponding giant magneto-amplification factor GMA is defined as

$$GMA = \frac{\beta(\text{parallel}) - \beta(\text{anti-parallel})}{\beta(\text{parallel})},$$
(61)

where (anti)parallel refers to the relative orientation of the equilibrium and nonequilibrium spins P_{0b} and δP_{e} .

Spin and magnetic control of current amplification would be optimized when the emitter efficiency dominates over base transport, as in Si-like transistors or specially tailored GaAs heterostructure transistors. In this case, we can neglect the factor $w_{\rm b}^2/2L_{\rm pb}^2$ in Equation (60) and write

$$\beta = \frac{j_{\rm gb}^{\rm ii}(\zeta_{\rm b})}{j_{\rm ge}^{\rm p}} (1 + \delta P_{\rm e} P_{\rm 0b}). \tag{62}$$

The relative change of β in a magnetic field or spin orientation change becomes

$$GMA = 2 \frac{|\delta P_{e} P_{0b}|}{1 + |\delta P_{e} P_{0b}|},$$
 (63)

which, for reasonable values of 50% spin polarizations would give a giant magneto-amplification of about 40%.

The above analysis of the forward active mode of an MBT should also apply to the reverse active mode, with the same proviso that the amplification is usually much smaller by design. The saturation mode of an MBT differs from that of a BJT. We have found that an MBT should be able to amplify signals also in this mode, solely due to spin-charge coupling, which should significantly enhance j_c over j_b [137]. If nonequilibrium spin is assumed to be added to both the emitter (δP_e) and the collector (δP_c) , one can show that it should be possible to control the current amplification by altering the difference of the two spin polarizations [137]:

$$\beta = \frac{P_{0b}(P_{0e} - P_{0c})}{w_b^2 / L_{nb}^2 + j_{ge}^p / j_{gb}^n + j_{gc}^p / j_{gb}^n} . \tag{64}$$

The current gain would be large because of the denominator, which contains the ratio of the hole to electron equilibrium densities. A remarkable aspect is that it should be possible to make the gain negative by switching from the emitter to collector spin polarization, or by changing the sign of the polarization.

It should also be possible to tune the ON and OFF logic states within this mode by spin-charge coupling. An MBT in the saturation mode should also act as a spin switch. In the cutoff mode, the MBT would be in the OFF state. Spin effects would be inhibited. We also include the spin-voltaic mode, in which $V_{be} = V_{bc} = 0$. A conventional BJT is in equilibrium, with no currents flowing, but an MBT would be active because of the presence of nonequilibrium spin. In this mode, $\delta n_{\rm be} = n_{\rm 0b} (\zeta_{\rm b}) \delta P_{\rm e} P_{\rm 0b}$, while the nonequilibrium hole densities should vanish. All of the activity would be controlled by spin-charge coupling. The transistor could act as a spin switch, changing the direction of the currents by changing the direction of spin. Unfortunately, the currents would be small, of the order of generation currents. Since only electrons would flow, $\gamma_e = 1$, and amplification in this mode could be very large, since it is solely due to α_t . These five modes are summarized in Table 1.

What is remarkable is that MA and GMA should not depend on spin relaxation in the base (typically much faster than the spin relaxation in the nonmagnetic regions). The controlling factor would be the carrier injection from the emitter into the base. Only spin relaxation in the depletion region between the emitter and base should be able to mask the effect. Fortunately, the depletion region would be rather small, especially in the forward bias, and the built-in electric field would cause fast spin drift. Magnetic bipolar transistors might also be used for electrical control of magnetism. In high injection limits (beyond the validity of our analytical theory),

where the number of injected electrons from the emitter to the base is comparable to the base doping density, the presence of free carriers should be able to induce ferromagnetism. Similar considerations would apply to small subregions of the depletion region. With increasing depletion, for example by reverse biasing, the subregions might lose their ferromagnetism, being void of free carriers. Such electrical control of ferromagnetism might be applicable to magnetic storage.

Concluding remarks

We have reviewed here both a theoretical framework for bipolar spin-polarized transport in semiconductors and several proposed device structures in which the contributions of both electrons and holes play important roles. By generalizing a concept of a p-n junction (a nonmagnetic diode) to include the effects of magnetism and nonequilibrium spin (injected by electrical or optical means), we have been led to several predictions. Circularly polarized light illuminating a p-n junction might be useful as a spin-polarized battery which would create a spin electromotive force and produce both spin and charge currents.

In the presence of a magnetic region, a nonequilibrium spin should lead to a spin-voltaic effect, a spin-analog of the photovoltaic effect. The direction of the charge current, which could flow even at no applied bias, could be switched by reversal of the equilibrium magnetization or by reversal of the polarization of the injected spin.

Our findings for p-n junctions can also be applied to more complicated multi-terminal geometries, in particular, to a *magnetic bipolar transistor*, which can be viewed as consisting of two magnetic p-n junctions connected in series. The spin-voltaic effect would then imply that by changing either the degree of injected nonequilibrium spin polarization or the spin-splitting of bands in one of the three regions (emitter, base, or collector), one could effectively control the gain or current amplification in such a device. We also predict the possibility of *giant magneto-amplification*, which could be viewed as a generalization of the spin-valve effect to semiconductor structures with strong intrinsic nonlinearities and thus possibly suitable for spin-enhanced logic applications.

Acknowledgments

We thank S. Das Sarma, M. Johnson, B. T. Jonker, H. Munekata, S. S. P. Parkin, A. Petukhov, and E. I. Rashba for useful discussions. This work was supported by the U.S. ONR, NSF, and DARPA. I. Žutić acknowledges financial support from the National Research Council. Use was made of resources of the Center for Computational Sciences at Oak Ridge

National Laboratory, which is supported by the Office of Science of the U.S. Department of Energy under Contract No. DE-AC05-00OR22725.

References and note

- S. Maekawa, S. Takahashi, and H. Imamura, in Spin Dependent Transport in Magnetic Nanostructures, S. Maekawa and T. Shinjo, Eds., Taylor and Francis, New York, 2002, pp. 143–236.
- S. S. P. Parkin, X. Jiang, C. Kaiser, A. Panchula, K. Roche, and M. Samant, *Proc. IEEE* 91, 661 (2003).
- 3. G. Prinz, Science 282, 1660 (1998).
- 4. J.-P. Ansermet, J. Phys.: Condens. Matter 10, 6027 (1998).
- 5. U. Hartman, Ed., Magnetic Multilayers and Giant Magnetoresistance, Springer, Berlin, 2000.
- E. Hirota, H. Sakakima, and K. Inomata, Giant Magneto-Resistance Devices, Springer, Berlin, 2002.
- J. Gregg, W. Allen, N. Viart, R. Kirschman, C. Sirisathitkul, J.-P. Schille, M. Gester, S. Thompson, P. Sparks, V. Da Costa, K. Ounadjela, and M. Skvarla, J. Magn. Magn. Mater. 175, 1 (1997).
- 8. M. Johnson, IEEE Spectrum 31, 47 (1994).
- J. S. Moodera and G. Mathon, J. Magn. Magn. Mater. 200, 248 (1999).
- S. S. P. Parkin, K. P. Roche, M. G. Samant, P. M. Rice, R. B. Beyers, R. E. Scheuerlein, E. J. O'Sullivan, S. L. Brown, J. Bucchignano, D. W. Abraham, Yu Lu, M. Rooks, P. L. Trouilloud, R. A. Wanner, and W. J. Gallagher, *J. Appl. Phys.* 85, 5828 (1999).
- S. Tehrani, B. Engel, J. M. Slaughter, E. Chen, M. DeHerrera, M. Durlam, P. Naji, R. Whig, J. Janesky, and J. Calder, *IEEE Trans. Magn.* 36, 2752 (2000).
- 12. M. Johnson, J. Supercond. 14, 273 (2001).
- I. Žutić, J. Fabian, and S. Das Sarma, Rev. Mod. Phys. 76, 323 (2004).
- S. Das Sarma, J. Fabian, X. Hu, and I. Žutić, *Solid State Commun.* 119, 207 (2001).
- 15. M. Tanaka, Semicond. Sci. Technol. 17, 327 (2002).
- V. N. Golovach and D. Loss, Semicond. Sci. Technol. 17, 355 (2002).
- M. Oestreich, M. Brender, J. Hübner, D. H. W. W. Rühle, T. H. P. J. Klar, W. Heimbrodt, M. Lampalzer, K. Voltz, and W. Stolz, Semicond. Sci. Technol. 17, 285 (2002).
- G. Schmidt and L. W. Molenkamp, Semicond. Sci. Technol. 17, 310 (2002).
- 19. H. Akinaga and H. Ohno, *IEEE Trans. Nanotech.* 1, 19 (2002).
- 20. S. von Molnár and D. Read, Proc. IEEE 91, 715 (2003).
- B. T. Jonker, S. C. Erwin, A. Petrou, and A. G. Petukhov, *Mater. Res. Soc. Bull.* 28, 740 (2003).
- 22. V. A. Sih, E. Johnston-Halperin, and D. D. Awschalom, *Proc. IEEE* **91**, 752 (2003).
- E. Yablonovitch, H. W. Jiang, H. Kosaka, H. D. Robinson,
 D. S. Rao, and T. Szkopek, *Proc. IEEE* 91, 761 (2003).
- I. Žutić, J. Fabian, and S. Das Sarma, *Phys. Rev. B* 64, 121201 (2001).
- I. Žutić, J. Fabian, and S. Das Sarma, *Phys. Rev. Lett.* 88, 066603 (2002).
- J. Fabian, I. Žutić, and S. D. Sarma, Appl. Phys. Lett. 84, 85 (2004).
- 27. I. Žutić, J. Fabian, and S. Erwin; see http://arxiv.org/abs/cond-mat/0412580 (2004).
- 28. See for example M. Johnson, Science 260, 320 (1993). In this paper, we use the term bipolar in the conventional sense. However, the term has also been used to describe an analogy between the coexistence of two spin-carrier populations (of spin-up and spin-down) in spin-polarized transport and two charge-carrier populations (electrons and holes) in bipolar charge transport.
- W. Shockley, Electrons and Holes in Semiconductors,
 D. Van Nostrand, Princeton, 1950.

- S. M. Sze, Physics of Semiconductor Devices, John Wiley, New York, 1981.
- F. Meier and B. P. Zakharchenya, Eds., Optical Orientation, North-Holland. New York. 1984.
- 32. G. Lampel, Phys. Rev. Lett. 20, 491 (1968).
- 33. A. I. Ekimov and V. I. Safarov, *Zh. Eksp. Teor. Fiz. Pisma Red.* **13**, 251 (1971); [*JETP Lett.* **13**, 177–179 (1971)].
- V. L. Vekua, R. I. Dzhioev, B. P. Zakharchenya, and V. G. Fleisher, *Fiz. Tekh. Poluprovodn.* 10, 354 (1976); [Sov. Phys. Semicond. 10, 210–212 (1976)].
- 35. W. G. Clark and G. Feher, Phys. Rev. Lett. 10, 134 (1963).
- A. G. Aronov, Zh. Eksp. Teor. Fiz. Pisma Red. 24, 37 (1976);
 [JETP Lett. 24, 32–34 (1976)].
- A. G. Aronov, Zh. Eksp. Teor. Fiz. 71, 370 (1976); [Sov. Phys. JETP 44, 193–196 (1976)].
- A. G. Aronov and G. E. Pikus, Fiz. Tekh. Poluprovodn. 10, 1177 (1976); [Sov. Phys. Semicond. 10, 698–700 (1976)].
- R. M. Stroud, A. T. Hanbicki, Y. D. Park, A. G. Petukhov, and B. T. Jonker, *Phys. Rev. Lett.* 89, 166602 (2002).
- 40. S. S. P. Parkin, C. Kaiser, A. Panchula, P. Rice, M. Samant, and S.-H. Yang, *Nature Mater.* 3, 862 (2004).
- W. H. Butler, X. Zhang, T. C. Schulthes, and J. M. MacLaren, *Phys. Rev. B* 63, 054416 (2001).
- 42. J. Mathon and A. Umerski, Phys. Rev. B 63, 220403 (2001).
- X. Jiang, R. Wang, R. M. Shelby, R. M. Macfarlane, S. R. Bank, J. S. Harris, and S. S. P. Parkin, *Phys. Rev. Lett.* 94, 056601 (2005).
- R. Wang, X. Jiang, R. M. Shelby, R. M. Macfarlane, S. S. P. Parkin, S. R. Bank, and J. S. Harris, *Appl. Phys. Lett.* 86, 052901 (2005).
- 45. I. Tsubokawa, J. Phys. Soc. Jpn. 15, 1664 (1960).
- 46. H. Munekata, H. Ohno, S. von Molnár, A. Segmüller, L. L. Chang, and L. Esaki, *Phys. Rev. Lett.* **63**, 1849 (1989).
- H. Ohno, H. Munekata, T. Penney, S. von Molnár, and L. L. Chang, *Phys. Rev. Lett.* 68, 2664 (1992).
- 48. H. Munekata, H. Ohno, R. R. Ruf, R. J. Gambino, and L. L. Chang, *J. Cryst. Growth* **111**, 1011 (1991).
- H. Ohno, A. Shen, F. Matsukura, A. Oiwa, A. End, S. Katsumoto, and Y. Iye, Appl. Phys. Lett. 69, 363 (1996).
- A. Van Esch, L. Van Bockstal, J. De Boeck, G. Verbanck,
 A. S. van Steenbergen, P. J. Wellmann, B. Grietens, R. Bogaerts,
 F. Herlach, and G. Borghs, *Phys. Rev. B* 56, 13103 (1997).
- T. Hayashi, M. Tanaka, T. Nishinaga, H. Shimada, T. Tsuchiya, and Y. Otuka, *J. Cryst. Growth* 175/176, 1063 (1997).
- H. Saito, W. Zaets, S. Yamagata, Y. Suzuki, and K. Ando, J. Appl. Phys. 91, 8085 (2002).
- H. Saito, V. Zayets, S. Yamagata, and K. Ando, *Phys. Rev. Lett.* 90, 207202 (2003).
- T. Dietl, H. Ohno, F. Matsukara, J. Cibert, and D. Ferrand, *Science* 287, 1019 (2000).
- T. Dietl, H. Ohno, and F. Matsukara, *Phys. Rev. B* 63, 195205 (2001).
- R. N. Bhat, M. Berciu, M. P. Kennett, and X. Wan, J. Supercond. 15, 71 (2002).
- 57. T. Dietl, Semicond. Sci. Technol. 17, 377 (2002).
- S. Sanvito, G. Theurich, and N. A. Hill, *J. Supercond.* 15, 85 (2002).
- S. Das Sarma, E. H. Hwang, and A. Kaminski, *Phys. Rev. B* 67, 155201 (2003).
- J. König, J. Schliemann, T. Jungwirth, and A. H. MacDonald, in *Electronic Structure and Magnetism* of Complex Materials, D. J. Singh and D. A. Papaconstantopoulos, Eds., Academic, New York, 2003, pp. 163–211.
- 61. C. Timm, J. Phys.: Condens. Matter 15, R1865 (2003).
- 62. S. C. Erwin and I. Žutić, Nature Mater. 3, 410 (2004).
- G. A. Medvedkin, T. Ishibashi, T. Nishi, K. Hayata, Y. Hasegawa, and K. Sato, *Jpn. J. Appl. Phys.*, *Part 2* 39, L949 (2000).
- S. Cho, S. Choi, G.-B. Cha, S. C. Hong, Y. Kim, Y.-J. Zhao,
 A. J. Freeman, J. B. Ketterson, B. J. Kim, Y. C. Kim, and
 B.-C. Choi, *Phys. Rev. Lett.* 88, 257203 (2002).

- 65. H. Ohno, Science 281, 951 (1998).
- 66. T. Dietl, Nature Mater. 2, 646 (2003).
- 67. N. Samarth, S. H. Chun, K. C. Ku, S. J. Potashnik, and P. Schiffer, *Solid State Commun.* 127, 173 (2003).
- Y. D. Park, A. T. Hanbicki, S. C. Erwin, C. S. Hellberg,
 J. M. Sullivan, J. E. Mattson, T. F. Ambrose, A. Wilson,
 G. Spanos, and B. T. Jonker, *Science* 295, 651 (2002).
- A. P. Li, J. Shen, J. R. Thompson, and H. H. Weitering, *Appl. Phys. Lett.* 86, 152507 (2005).
- S. Koshihara, A. Oiwa, M. Hirasawa, S. Katsumoto, Y. Iye,
 S. Urano, H. Takagi, and H. Munekata, *Phys. Rev. Lett.* 78, 4617 (1997).
- A. Oiwa, Y. Mitsumori, R. Moriya, T. Supinski, and H. Munekata, *Phys. Rev. Lett.* 88, 137202 (2002).
- H. Ohno, D. Chiba, F. Matsukura, T. O. E. Abe, T. Dietl, Y. Ohno, and K. Ohtani, *Nature* 408, 944 (2000).
- J. De Boeck, R. Oesterholt, A. Van Esch, H. B. R. C. Bruynseraede, C. Van Hoof, and G. Borghs, *Appl. Phys. Lett.* 68, 2744 (1996).
- S. J. Pearton, C. R. Abernathy, M. E. Overberg, G. T. Thaler, D. P. Norton, N. Theodoropoulou, A. F. Hebard, Y. D. Park, F. Ren, J. Kim, and L. A. Boatner, *J. Appl. Phys.* 93, 1 (2003).
- D. P. Young, D. Hall, M. E. Torelli, Z. Fisk, J. L. Sarrao, J. D. Thompson, H.-R. Ott, S. B. Oseroff, R. G. Goodrich, and R. Zysler, *Nature* 397, 412 (1999).
- H. R. Ott, J. L. Gavilano, B. Ambrosini, P. Vonlanthen,
 E. Felder, L. Degiorgi, D. P. Young, Z. Fisk, and R. Zysler,
 Physica B 281/282, 423 (2000).
- H. J. Tromp, P. van Gelderen, P. J. Kelly, G. Brocks, and P. A. Bobbert, *Phys. Rev. Lett.* 87, 016401 (2001).
- M. C. Bennett, J. van Lierop, E. M. Berkeley, J. F. Mansfield, C. Henderson, M. C. Aronson, D. P. Young, A. Bianchi, Z. Fisk, F. Balakirev, and A. Lacerda, *Phys. Rev. B* 69, 132407 (2004).
- B. T. Jonker, A. T. Hanbicki, D. T. Pierece, and M. D. Stiles, J. Magn. Magn. Mater. 277, 24 (2004).
- 80. M. A. M. Gijs and G. E. W. Bauer, Adv. Phys. 46, 285 (1997).
- 81. M. Johnson and R. H. Silsbee, Phys. Rev. B 37, 5312 (1988).
- 82. M. D. Stiles and A. Zangwill, Phys. Rev. B 66, 014407 (2002).
- 83. S. Hershfield and H. L. Zhao, Phys. Rev. B 56, 3296 (1997).
- 84. E. I. Rashba, Eur. Phys. J. B 29, 513 (2002).
- S. Takahashi and S. Maekawa, *Phys. Rev. B* 67, 052409 (2003).
- J. Fabian, I. Žutić, and S. Das Sarma, *Phys. Rev. B* 66, 165301 (2002).
- 87. N. W. Ashcroft and N. D. Mermin, *Solid State Physics*, Sounders, Philadelphia, 1976.
- 88. I. Žutić, J. Fabian, and S. Das Sarma, *Appl. Phys. Lett.* **79**, 1558 (2001)
- I. Žutić, J. Fabian, and S. Das Sarma, Appl. Phys. Lett. 82, 221 (2003).
- D. J. Hilton and C. L. Tang, *Phys. Rev. Lett.* 89, 146601 (2002).
- 91. R. R. Parsons, Phys. Rev. Lett. 23, 1152 (1969).
- M. I. D'yakonov and V. I. Perel', Zh. Eksp. Teor. Fiz. Pisma Red. 13, 206 (1971); [JETP Lett. 13, 144–146 (1971)].
- R. I. Dzhioev, B. P. Zakharchenya, V. L. Korenev, and M. N. Stepanova, *Fiz. Tverd. Tela* 39, 1975 (1997); [*Phys. Solid State* 39, 1765–1768 (1997)].
- J. M. Kikkawa and D. D. Awschalom, *Phys. Rev. Lett.* 80, 4313 (1998).
- R. I. Dzhioev, B. P. Zakharchenya, V. L. Korenev, D. Gammon, and D. S. Katzer, *Zh. Eksp. Teor. Fiz. Pisma Red.* 74, 182 (2001); [*JETP Lett.* 74, 200–203 (2001)].
- Y. V. Pershin and V. Privman, *Phys. Rev. Lett.* **90**, 256602 (2003).
- I. Malajovich, J. J. Berry, N. Samarth, and D. D. Awschalom, *Nature* 411, 770 (2001).
- 98. S. Datta, Appl. Phys. Lett. 87, 013115 (2005).
- S. D. Ganichev and W. Prettl, J. Phys.: Condens. Matter 15, R935 (2003).

- W. Long, Q.-F. Sun, H. Guo, and J. Wang, *Appl. Phys. Lett.* 83, 1397 (2003).
- A. G. Mal'shukov, C. S. Tang, C. S. Chu, and K. A. Chao, *Phys. Rev. B* 68, 233307 (2003).
- 102. J. K. Furdyna, J. Appl. Phys. 64, R29 (1988).
- T. Dietl, in *Handbook of Semiconductors*, Vol. 3, T. S. Moss and S. Mahajan, Eds., North-Holland, New York, 1994, p. 1251.
- 104. M. A. Zudov, J. Kono, Y. H. Matsuda, T. Ikaida, N. Miura, H. Munekata, G. D. Sanders, Y. Sun, and C. J. Stanton, *Phys. Rev. B* 66, 161307 (2002).
- M. Deutsch, G. Vignale, and M. F. Flatté, J. Appl. Phys. 96, 7424 (2004).
- D. Schmeltzer, A. Saxena, A. Bishop, and D. L. Smith, *Phys. Rev. B* 68, 195317 (2003).
- J. Stephens, J. Berezovsky, J. P. McGuire, L. J. Sham, A. C. Gossard, and D. D. Awschalom, *Phys. Rev. Lett.* 93, 097602 (2004).
- A. M. Bratkovsky and V. V. Osipov, J. Appl. Phys. 96, 4525 (2004).
- 109. R. H. Silsbee, Bull. Magn. Reson. 2, 284 (1980).
- M. Johnson and R. H. Silsbee, *Phys. Rev. Lett.* 55, 1790 (1985).
- 111. I. Žutić and J. Fabian, Mater. Trans. JIM 44, 2062 (2003).
- N. Nakagawa, M. Asai, Y. Mukunoki, T. Susaki, and H. Y. Hwang, Appl. Phys. Lett. 86, 082504 (2005).
- J. Hayafuji, T. Kondo, and H. Munekata, Inst. Phys. Conf. Series 184, 127 (2005).
- H. Munekata, in Concepts in Spin Electronics, S. Maekawa, Ed., Oxford University Press, New York, 2005.
- 115. C. P. Wen, B. Hershenov, H. von Philipsborn, and H. L. Pinch, *IEEE Trans. Magn.* 4, 702 (1968).
- E. Janik and G. Karczewski, *Acta. Phys. Polon. A* 73, 439 (1988).
- Y. Ohno, I. Arata, F. Matsukura, K. Ohtani, S. Wang, and H. Ohno, *Appl. Surf. Sci.* **159-160**, 308 (2000).
- M. Kohda, Y. Ohno, K. Takamura, F. Matsukura, and H. Ohno, *Jpn. J. Appl. Phys.* 40, L1274 (2001).
- E. Johnston-Halperin, D. Lofgreen, R. K. Kawakami, D. K. Young, L. Coldren, A. C. Gossard, and D. D. Awschalom, *Phys. Rev. B* 65, 041306 (2002).
- I. Arata, Y. Ohno, F. Matsukura, and H. Ohno, *Phys. E* 10, 288 (2001).
- 121. P. Van Dorpe, Z. Liu, W. V. Roy, V. F. Motsnyi, M. Sawicki, G. Borghs, and J. De Boeck, *Appl. Phys. Lett.* 84, 3495 (2004).
- 122. F. Tsui, L. Ma, and L. He, Appl. Phys. Lett. 83, 954 (2003).
- R. Fiederling, M. Kleim, G. Reuscher, W. Ossau, G. Schmidt, A. Waag, and L. W. Molenkamp, *Nature* 402, 787 (1999).
- B. T. Jonker, Y. D. Park, B. R. Bennett, H. D. Cheong, G. Kioseoglou, and A. Petrou, *Phys. Rev. B* 62, 8180 (2000).
- D. K. Young, E. Johnston-Halperin, D. D. Awschalom,
 Y. Ohno, and H. Ohno, Appl. Phys. Lett. 80, 1598 (2002).
- 126. A. Hanbicki, O. M. J. van t'Erve, R. Magno, G. Kioseoglou, C. H. Li, B. T. Jonker, G. Itskos, R. Mallory, M. Yasar, and A. Petrou, Appl. Phys. Lett. 82, 4092 (2003).
- 127. X. Jiang, R. Wang, S. van Dijken, R. Shelby, R. Macfarlane, G. S. Solomon, J. Harris, and S. S. P. Parkin, *Phys. Rev. Lett.* 90, 256603 (2003).
- 128. J. Rudolph, D. Hägele, H. M. Gibbs, G. Khitrova, and M. Oestreich, *Appl. Phys. Lett.* **82**, 4516 (2003).
- W. Shockley, M. Sparks, and G. K. Teal, *Phys. Rev.* 83, 151 (1951).
- 130. J. Fabian and I. Žutić, Phys. Rev. B 69, 115314 (2004).
- 131. J. Fabian and I. Žutić, Appl. Phys. Lett. 86, 133506 (2005).
- 132. S. Dimitrijev, *Understanding Semiconductor Devices*, Oxford University Press, New York, 2000.
- J. Fabian, I. Žutić, and S. Das Sarma, see <a href=http://arxiv/org/abs/cond-mat/0211639 (2002).
- N. Lebedeva and P. Kuivalainen, J. Appl. Phys. 93, 9845 (2003).

- 135. M. E. Flatté, Z. G. Yu, E. Johnston-Halperin, and D. D. Awschalom, *Appl. Phys. Lett.* **82**, 4740 (2003).
- S. Bandyopadhyay and M. Cahay, Appl. Phys. Lett. 86, 133502 (2005).
- 137. J. Fabian and I. Žutić, Acta Phys. Polon. A 106, 109 (2004).

Received April 22, 2005; accepted for publication September 21, 2005; Internet publication February 3, 2006

Igor Žutić Department of Physics, State University of New York at Buffalo, Buffalo, New York 14260 (zigor@buffalo.edu). Dr. Zutic received his Ph.D. degree in physics from the University of Minnesota in 1998, working on high-temperature superconductors. After holding a postdoctoral appointment at the University of Maryland and a National Research Council Fellowship at the U.S. Naval Research Laboratory, he joined the University of New York at Buffalo in 2005 as an Assistant Professor of Physics. His current interests involve spin-polarized transport in electronic materials, novel spin-based devices, ferromagnetic semiconductors, and high-temperature superconductors.

Jaroslav Fabian *Institute for Theoretical Physics*, University of Regensburg 93040 Regensburg, Germany (jaroslav.fabian@physik.uni-regensburg.de). Dr. Fabian is a Professor of Theoretical Physics at the University of Regensburg. He received a master's degree in mathematical physics from Comenius University in Bratislava, Slovakia, and a Ph.D. degree in physics in 1997 from the State University of New York at Stony Brook. He was subsequently a Research Associate at the University of Maryland in College Park, where he began his work on spintronics. In 2000, he joined the staff of the Max-Planck Institute for Complex Systems in Dresden, Germany, and in 2001 became an Assistant Professor at the Institute for Theoretical Physics at the Karl-Franzens University Graz, Austria. In 2004, Dr. Fabian became an Associate Professor and in December 2004 joined the faculty of the University of Regensburg as a University Professor. His current interests are in spin-polarized transport in semiconductors, spintronic devices, nanospintronics, and spinbased quantum information processing.

Steven C. Erwin Center for Computational Materials Science, U.S. Naval Research Laboratory, Washington, DC 20375 (Steven.Erwin@nrl.navy.mil). Dr. Erwin is a Research Physicist in the Materials Science and Technology Directorate at the Naval Research Laboratory (NRL). He received an A.B. degree in physics from Harvard University in 1982, and M.S. and Ph.D. degrees in physics from the University of Wisconsin at Madison in 1984 and 1988, respectively. He came to NRL in 1988 as a National Research Council Postdoctoral Fellow and completed a second postdoctoral position at the University of Pennsylvania before returning to NRL in 1994 as a Staff Member. Dr. Erwin's current research interests include ferromagnetic semiconductors, surface physics, and nanocrystals. He is an author or coauthor of 90 technical papers.